Journal Pre-proofs

Multivariate GR&R through Factor Analysis

Rafaela Aparecida Mendonça Marques, Robson Bruno Dutra Pereira, Rogério Santana Peruchi, Lincoln Cardoso Brandão, João Roberto Ferreira, J. Paulo Davim

Please cite this article as: R. Aparecida Mendonça Marques, R. Bruno Dutra Pereira, R. Santana Peruchi, L. Cardoso Brandão, J. Roberto Ferreira, J. Paulo Davim, Multivariate GR&R through Factor Analysis, *Measurement* (2019), doi: https://doi.org/10.1016/j.measurement.2019.107107

Multivariate GR&R through Factor Analysis

Rafaela Aparecida Mendonça Marques[1], Robson Bruno Dutra Pereira[1,4*], Rogério Santana Peruchi[2], Lincoln Cardoso Brandão[1], João Roberto Ferreira[3], J. Paulo Davim[4]

Corresponding author: * robsondutra@ufsj.edu.br, +55 32 9140-9788

[1] Department of Mechanical Engineering, Federal University of São João Del-Rei,

170 Frei Orlando Square, São João del Rei, MG 36880000, Brazil

[2] Production Engineering Department, Federal University of Paraíba, João Pessoa, PB, Brazil

[3] Institute of Industrial Engineering and Management, Federal University of Itajubá, 1303 BPS Avenue, Itajubá, MG 37500-903, Brasil

[4] Department of Mechanical Engineering, University of Aveiro, Campus Santiago, 3810-193 Aveiro, Portugal

Abstract

Several measurement tasks present multivariate nature. In the cases with quality characteristics highly correlated within groups, but with a relatively small correlation between groups, the available multivariate GR&R methods are not suitable to provide a correct interpretation of the results. The present work presents a new multivariate GR&R approach through factor analysis. Factor analysis is a multivariate statistical method which focuses on the explanation of the covariance structure of the data. Through orthogonal rotation of the factors a suitable structure can be achieved with loadings easy to relate the variables to the factors. The proposed multivariate GR&R method through factor analysis is described and applied in the quality evaluation of holes obtained through helical milling process of AISI H13 hardened steel. The method succeeded in achieving a simple structure, with one factor related to the roughness outcomes and other related to the roundness ones, simplifying the gage capability evaluation.

Keywords

Multivariate GR&R, factor analysis, helical milling, roughness, roundness

1 INTRODUCTION

Planning, designing, running and controlling modern industrial processes have been a tough task. A lot of data and information have been generated, and turning them into knowledge requires advanced methods [1–3]. In statistical quality control (SQC), current researches have been conducted applying data mining tools, Markov chains, multivariate control charts, advanced process capability

analyses, and so on [1,3]. Before any of these statistical data analyses be conducted, the analyst must assure that the dataset is reliable [4,5]. Measurement system analysis (MSA) is another essential SQC technique, which was conceived to evaluate measurement errors. Such errors may come from random and/or systematic sources of variation. Dealing with random errors, Gage Repeatability, and Reproducibility (GR&R) is the most used technique [2,5,6]. AIAG [7] states that repeatability is the variation "within the system" when measurement conditions are fixed - part, operator, instrument, time, standard, method, environmental conditions, etc. Reproducibility can be stated as the variation "between systems" or between measurement conditions - instruments, laboratories, environmental conditions and, mainly, operators.

As mentioned above, in modern manufacturing processes, to attain reliable measurements is an even more important issue. For such complex measurement systems, current researches have been conducted by using multivariate methods such as principal component analysis (PCA) [5,6,8–10] and multivariate analysis of variance (MANOVA) [2,4–6,8]. Several measurement tasks present multivariate nature since some products can only be completely characterized by the measurement of distinct quality characteristics. The main goal in the application of multivariate analysis in measurement results is to threat the linear dependence or correlation among the variables, besides reducing the redundancy among them. When the analyst neglects the correlation structure conducting individual univariate analysis for each variable, he/she incurs in making a wrong decision since part of data variability is related to the common variance between each pair of variables. In the case of GR&R assignments, a wrong decision may entail in the application of an unable measurement system to quality control.

Some recent works proposed GR&R multivariate approaches. Majeske [4] proposed a multivariate GR&R study based on MANOVA. In an automotive gage study, this multivariate approach not only provided a better model for measurement errors but also determined a more reliable assessment for the measurement system. Another significant method based on MANOVA was proposed by Peruchi et al. [2]. Estimating the multivariate evaluation index, the authors showed that weighted approaches were more successful in evaluating multivariate measurement systems.

Applying PCA method, Wang and Yang [11] and Wang and Chien [10] showed the effectiveness of multivariate approaches when correlated quality characteristics are assessed in GR&R studies. The authors have proved their results by comparing univariate and multivariate methods. Some interesting findings were provided by Peruchi et al. [12] and Peruchi et al. [6]. The authors demonstrated that, among the multivariate methods, weighted approaches determined better estimates for multivariate measurement system indexes.

The aforementioned multivariate methods are adequate to model the variance-covariance structure among several quality characteristics. However, complex systems usually demand several measuring devices for process control. In such conditions, the covariance relationship might be more important than the variance for measurement system analysis. Dealing with variables highly correlated within a group, but with a relatively small correlation between other groups is a more suitable task to factor analysis (FA) [13,14]. Thus, this research aims to propose a new multivariate GR&R study to explain the covariance structure among several quality characteristics. FA and GR&R methods are used to assess complex systems with multiple measuring devices. An application of helical milling process of AISI H13 hardened steel workpieces is performed. A measurement system considering microgeometrical (R_a, R_q, and R_z roughness parameters) and geometrical (Ron_p and Ron_t roundness parameters and Cyl_t total cylindricity) quality characteristics are assessed. The results have shown that the proposed method is very successful in assessing the multivariate measurement system with multiple quality characteristics, which were measured by multiple measuring devices.

The remaining sections of this paper are structured as follows. Sections 2 and 3 present a literature review on GR&R and FA methods. Section 4 details the proposed GR&R-FA method. Section 5 introduces the experimental application of the multivariate measurement system. Section 6 shows how to apply the proposed method into manufacturing systems with multiple measuring devices. Finally, the main findings of this research are summarized in section 7.

2   CROSSED GR&R STUDY

A crossed GR&R study is a factorial design intended to study the sources of variability which affects a measurement system. Crossed GR&R studies are considered factorial experiments, since each operator measures each part r times, i.e., each level of one factor is performed in each level of the other factor r times [15]. It is also usual to perform a GR&R study considering other variability sources apart from operators and parts, such as the measurement instrument, also referred to expanded GR&R studies. Logically, all the combinations of the levels may be performed to guarantee a crossed GR&R study. In the cases where the measurements for each operator cannot be done in the same parts, such as in the destructive measurements, a nested structure may be considered [16].

In a crossed GR&R study the factors are generally considered random. When limited levels of factors are chosen randomly aiming to achieve conclusions for all the population of levels, the factors are said to be random [17].

The ANOVA model of a crossed GR&R study with p parts, o operators and r replicates can be written as follows:

$$y_{ijk} = \mu + P_i + O_j + (PO)_{ij} + \varepsilon_{ijk} \begin{cases} i = 1,...,p \\ j = 1,...,o \\ k = 1,...,r \end{cases} \tag{1}$$

where μ is the mean of the measured values, P_i, O_j, $(PO)_{ij}$, and ε_{ijk} are jointly independent normal random variables with means zero and variances σ_P^2, σ_O^2, σ_{PO}^2, and σ_ε^2, for part-to-part variation, operator, part*operator interaction and the error term, respectively [15]. The components of variance in Eq. (1) can be estimated according to the equations in Table 1. If the interaction term (PO) is insignificant, this component is removed from the model and the denominator of $F_{0(P)}$ and $F_{0(O)}$ statistics would replace σ_{PO}^2 by σ_ε^2.

Table 1. ANOVA table for a crossed GR&R study with two random factors

Sources	Degrees of freedom	Mean square	F_0
Parts (P)	$p - 1$	$\sigma_P^2 = \dfrac{or\Sigma_i(\bar{y}_{i..} - \bar{y}_{...})^2}{p - 1}$	$F_{0(P)} = \dfrac{\sigma_P^2}{\sigma_{PO}^2}$
Operators (O)	$o - 1$	$\sigma_O^2 = \dfrac{pr\Sigma_j(\bar{y}_{.j.} - \bar{y}_{...})^2}{o - 1}$	$F_{0(O)} = \dfrac{\sigma_O^2}{\sigma_{PO}^2}$
$P \times O$	$(p - 1)(o - 1)$	$\sigma_{PO}^2 = \dfrac{r\Sigma_i\Sigma_j(\bar{y}_{ij.} - \bar{y}_{i..} - \bar{y}_{.j.} + \bar{y}_{...})^2}{(p - 1)(o - 1)}$	$F_{0(PO)} = \dfrac{\sigma_{PO}^2}{\sigma_\varepsilon^2}$
Repeatability (ε)	$po(r - 1)$	$\sigma_\varepsilon^2 = \dfrac{\Sigma_i\Sigma_j\Sigma_k(y_{ijk} - \bar{y}_{ij.})^2}{po(r - 1)}$	

where $\bar{y}_{...}$ is the grand mean of the measurements; $\bar{y}_{i..}$ is the average of the ith part; $\bar{y}_{.j.}$ is the average of the jth operator; $\bar{y}_{ij.}$ is the average of the ith part measured by the jth operator and y_{ijk} is the kth measurement of the ith part by the jth operator

One of the main objectives of the crossed GR&R study is to identify the sources of variation of the measurement system. The experimental total variance is expressed by Eq. 2 [15,17].

$$\hat{\sigma}_T^2 = \hat{\sigma}_P^2 + \hat{\sigma}_{R\&R}^2 \tag{2}$$

where $\hat{\sigma}_P^2$ is the process variance estimated by Eq. 3 and $\hat{\sigma}_{R\&R}^2$ is the measurement system variance, calculated by Eq. 4.

$$\hat{\sigma}_P^2 = \frac{\sigma_P^2 - \sigma_{PO}^2}{or} \tag{3}$$

$$\hat{\sigma}_{R\&R}^2 = \hat{\sigma}_\varepsilon^2 + \hat{\sigma}_{Reproducibility}^2 \tag{4}$$

where $\hat{\sigma}_\varepsilon^2 = S_\varepsilon^2$ is the variance due to repeatability and the variance due to reproducibility is $\hat{\sigma}_{Reproducibility}^2 = \hat{\sigma}_O^2 + \hat{\sigma}_{PO}^2$. Reproducibility is composed by operator and part*operator interaction components, which are calculated by Eqs. 5 and 6, respectively.

$$\hat{\sigma}_O^2 = \frac{\sigma_O^2 - \sigma_{PO}^2}{pr} \tag{5}$$

$$\hat{\sigma}_{PO}^2 = \frac{\sigma_{PO}^2 - \sigma_\varepsilon^2}{r} \tag{6}$$

According to AIAG [7] criteria, the main classification index for assessing measurement system adequacy is the %R&R (percentage of repeatability and reproducibility). Basically, this index is about comparing measurement system variation to the total variation, as such the Eq. 7:

$$\%R\&R = \frac{\hat{\sigma}_{R\&R}}{\hat{\sigma}_T} \tag{7}$$

As shown in Fig. 1, the measurement system is acceptable if $\%R\&R < 0.10$. In some applications a marginal measurement system, with $0.10 < \%R\&R < 0.30$ can be tolerable. %R&R>0.30 determines that the measurement system is unacceptable and must be improved.

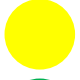|	
Unacceptable	%R&R > 30%
Marginal	10% < %R&R < 30%
Acceptable	%R&R < 10%

Fig. 1. GR&R criteria for measurement system acceptability [7,18]

According to [19], some additional indices for assessing measurement system adequacy can be estimated. Comparing the measurement system variation to the process tolerance (T), the precision-to-tolerance ratio (PTR) index is calculated as follows:

$$PTR = \frac{6\hat{\sigma}_{R\&R}}{T} \tag{8}$$

The criteria for measurement system acceptance, based on *PTR* index, are the same as those on Fig. 1. Relating signal (process variation) to noise (measurement error), the signal-to-noise ratio (SNR) (or ndc, number of distinct categories) can also be utilized for measurement system assessment. This index is calculated as follows:

$$SNR = \frac{\sqrt{2}\hat{\sigma}_P}{\hat{\sigma}_{R\&R}} \tag{9}$$

SNR greater than four is usually required for measurement system acceptance. *SNR* lower than two would classify the measurement system as unacceptable. An alternative to *SNR* is the discriminant ratio (DR) ratio, which is expressed as:

$$DR = \sqrt{\frac{2\hat{\sigma}_P^2}{\hat{\sigma}_{R\&R}^2} + 1} \tag{10}$$

If $DR \geq 4$, the measurement system is deemed acceptable. On the other hand, if $DR < 2$, the measurement system is unacceptable. Finally, if $2 < DR \leq 4$, the measurement system is marginal [19,20].

3 FACTOR ANALYSIS

Factor analysis is a branch of multivariate statistics originally developed by psychologists to deal with hypothesis on the mental abilities considering the correlation structure of cognitive tests variates [21]. Spearman [22] introduced the factor analysis to relate six intellectual test variables to only one latent variable. Thurstone [23] generalized the Spearman model taking into consideration multiple latent variables, for the first time named factors. The early association with intelligence scores explains why the factor analysis was initially proposed and developed by researchers in psychometrics. The advent of the computers allowed the development of factor analysis as a multivariate statistical analysis method, with most of the controversies solved [14,24]. Factor analysis is yet widely applied as multivariate analysis method in the psychology field, but the recent advances helped to disseminate the method to other fields such as biology, social sciences, economics [21] and lately in engineering [25–29]. In factor analysis, each variable is described as a linear function in terms of common factors and specific factors. The common factors explain the

variances and covariances, while the specific factors explain only the variances of the original variables [24].

The purpose of the factor analysis is to describe the covariance structure among $y_1, y_2, \ldots, y_p$ variables in terms of few implicit and unobservable quantities called factors $f_1, f_2, \ldots, f_m, m < p$. The factors are latent variables which generate the variables $y_1, y_2, \ldots, y_p$. If these variables are moderately correlated, the dimension of the system is considerably lower than p. Therefore, it is desired to deal with the redundancy among the variances using only few factors, i.e., $m \ll p$. The factor analysis presents the of approximate the covariance matrix $\boldsymbol{\Sigma}$, focusing more in the covariances than in the variances explanation, being helpful in dealing with groups of highly correlated variables [14].

In factor analysis, only $m < p$ factors are necessary to explain the covariance structure. However, the total explanation of the variance provided by m factors is in general not perfect. Another specificity is that in factor analysis the problem of parameter identification of the factor model should be overcome since the solution is not unique. However, the non-singularity may be used positively, since when rotating the factors in distinct ways, it may be achieved a better interpretation of them [24].

Assuming that the pattern of the correlation matrix is such that there are subsets of variables with high correlation between them, but with low correlation with variables of other subsets. Is this case it may have a factor which could be responsible by the correlations in each highly correlated subset [13,14].

This intrinsic partitioning of the factor analysis is of great interest in manufacturing process control, modeling, and optimization. Several processes may present different subsets of quality characteristics highly correlated between them which could be described by factors. Consequently, the redundancy among the variables may be reduced, facilitating the analysis.

Consider a random vector $\boldsymbol{Y}$ with p variables, a random sample $\boldsymbol{Y}_1, \boldsymbol{Y}_2, \ldots, \boldsymbol{Y}_N$ with mean vector $\boldsymbol{\mu}$ and covariance matrix $\boldsymbol{\Sigma}$, as follows:

$$\boldsymbol{Y} = \begin{bmatrix} Y_1 \\ Y_2 \\ \vdots \\ Y_p \end{bmatrix}; \qquad \boldsymbol{\mu} = \begin{bmatrix} E(Y_1) \\ E(Y_2) \\ \vdots \\ E(Y_p) \end{bmatrix} = \begin{bmatrix} \mu_1 \\ \mu_2 \\ \vdots \\ \mu_p \end{bmatrix}; \qquad \boldsymbol{\Sigma} = \begin{bmatrix} \sigma_{11} & \sigma_{12} & \ldots & \sigma_{1p} \\ \sigma_{21} & \sigma_{22} & \ldots & \sigma_{2p} \\ \vdots & \vdots & \ddots & \vdots \\ \sigma_{p1} & \sigma_{p2} & \ldots & \sigma_{pp} \end{bmatrix}$$

For an arbitrary observation $Y_1, Y_2, \ldots, Y_p$, the factor model may be described as follows [13,14,24]:

$$Y_1 - \mu_1 = l_{11}F_1 + l_{12}F_2 + ... + l_{1j}F_j + ... + l_{1m}F_m + \varepsilon_1$$
$$Y_2 - \mu_2 = l_{21}F_1 + l_{22}F_2 + ... + l_{2j}F_j + ... + l_{2m}F_m + \varepsilon_2$$
$$\vdots$$
$$Y_i - \mu_i = l_{i1}F_1 + l_{i2}F_2 + ... + l_{ij}F_j + ... + l_{im}F_m + \varepsilon_i \qquad (7)$$
$$\vdots$$
$$Y_p - \mu_p = l_{p1}F_1 + l_{p2}F_2 + ... + l_{pj}F_j + ... + l_{pm}F_m + \varepsilon_p$$

The p deviations $Y_i - \mu_i$, $i = 1, …, p$ are expressed in terms of $p + m$ random variables F_1, F_2, ..., F_m, ε_1, ε_2, ..., ε_p which are non-observable, with $i = 1, …, p$ and $j = 1, …, m$. The coefficient l_{ij} is the factor loading of the i-th variable in the j-th factor and represents the degree of relationship between Y_i and F_j. Therefore, in factor analysis, the original variables are described through linear combinations of the factors [24]. In matrix notation, the model in Eq. 7 can be expressed as follows:

$$Y - \mu = LF + \varepsilon \qquad (8)$$

In the Eq. 8 of the orthogonal factor model, L is a matrix of factor loadings of order $p \times m$, $m < p$, F is a matrix of order $m \times 1$ of the common factors, which are non-observable latent variables, and ε is a vector of random error of order $p \times 1$ [24], as follows:

$$Y - \mu = \begin{bmatrix} Y_1 - \mu_1 \\ Y_2 - \mu_2 \\ \vdots \\ Y_p - \mu_p \end{bmatrix}; \quad L = \begin{bmatrix} l_{11} & l_{12} & ... & l_{1m} \\ l_{21} & l_{22} & ... & l_{2m} \\ \vdots & \vdots & \ddots & \vdots \\ l_{p1} & l_{p2} & ... & l_{pm} \end{bmatrix}; \quad F = \begin{bmatrix} F_1 \\ F_2 \\ \vdots \\ F_p \end{bmatrix}; \quad \varepsilon = \begin{bmatrix} \varepsilon_1 \\ \varepsilon_2 \\ \vdots \\ \varepsilon_p \end{bmatrix} \qquad (9)$$

Since F is non-observable, the model of the Eq. 8 is different from a multivariate regression model, in which the independent variables may be observable. Some assumptions should be satisfied for the orthogonal factor model: $E(Y) = \mu$, $E(F) = E(\varepsilon) = 0$, $Cov(F) = I_{(m \times m)}$, $Cov(Y) = \Sigma_{(p \times p)}$, $Cov(\varepsilon) = \Psi_{(p \times p)}$ e $Cov(F, \varepsilon) = 0_{(m \times p)}$ [13,14,24], where:

$$\Psi = \begin{bmatrix} \psi_1 & 0 & ... & 0 \\ 0 & \psi_2 & ... & 0 \\ \vdots & \vdots & \ddots & \vdots \\ 0 & 0 & ... & \psi_p \end{bmatrix} \qquad (10)$$

with $\psi_i > 0$, $i = 1, 2, ..., p$. These assumptions imply that the errors are not correlated among them and that, not necessarily, present equal variances. The model in Eq. 8 supported by these

assumptions is the factor model, with m orthogonal factors among themselves, i.e., not correlated, which implies a covariance structure for $\mathbf{Y}$. From the model in Eq. 8 [14,24]:

$$(\boldsymbol{Y} - \boldsymbol{\mu})(\boldsymbol{Y} - \boldsymbol{\mu})^T = (\boldsymbol{LF} + \boldsymbol{\varepsilon})(\boldsymbol{LF} + \boldsymbol{\varepsilon})^T$$
$$(\boldsymbol{Y} - \boldsymbol{\mu})(\boldsymbol{Y} - \boldsymbol{\mu})^T = (\boldsymbol{LF})(\boldsymbol{LF})^T + (\boldsymbol{LF})\boldsymbol{\varepsilon}^T + \boldsymbol{\varepsilon}(\boldsymbol{LF})^T + \boldsymbol{\varepsilon}(\boldsymbol{\varepsilon})^T \tag{11}$$

Therefore, the covariance structure of the orthogonal model in Eq. 8 can be described as [14,24]:

$$Cov(\boldsymbol{Y}) = \boldsymbol{\Sigma} = E(\boldsymbol{Y} - \boldsymbol{\mu})(\boldsymbol{Y} - \boldsymbol{\mu})^T = E(\boldsymbol{LF} + \boldsymbol{\varepsilon})(\boldsymbol{LF} + \boldsymbol{\varepsilon})^T$$
$$Cov(\boldsymbol{Y}) = E\left[(\boldsymbol{LF})(\boldsymbol{LF})^T\right] + E\left[(\boldsymbol{LF})\boldsymbol{\varepsilon}^T\right] + E\left[\boldsymbol{\varepsilon}(\boldsymbol{LF})^T\right] + E\left[\boldsymbol{\varepsilon}\boldsymbol{\varepsilon}^T\right]$$
$$Cov(\boldsymbol{Y}) = \boldsymbol{L}E\left(\boldsymbol{FF}^T\right)\boldsymbol{L}^T + \boldsymbol{L}E\left(\boldsymbol{F}\boldsymbol{\varepsilon}^T\right) + E(\boldsymbol{\varepsilon}\boldsymbol{F})^T\boldsymbol{L}^T + \boldsymbol{\Psi}$$
$$Cov(\boldsymbol{Y}) = \boldsymbol{LIL}^T + \boldsymbol{L0} + \boldsymbol{0L}^T + \boldsymbol{\Psi}$$
$$Cov(\boldsymbol{Y}) = \boldsymbol{\Sigma} = \boldsymbol{LL}^T + \boldsymbol{\Psi} \tag{12}$$

or explicitly

$$\begin{aligned} Var(Y_i) &= \sigma_{ii} = l_{i1}^2 + l_{i2}^2 + \cdots + l_{im}^2 + \psi_i \\ Cov(Y_i, Y_k) &= \sigma_{ik} = l_{i1}l_{k1} + l_{i2}l_{k2} + \cdots + l_{im}l_{km} \end{aligned} \tag{13}$$

The variance portion of the i-th variable in the j-th common factor is called commonality or common variance. These elements are located in the diagonal of $\boldsymbol{LL}^T$ and are defined as the sum of squares of the loadings of the i-th variable in the m common factors, according to Eq. 14 [14,24].

$$h_i^2 = \sum_{j=1}^m l_{ij}^2 = l_{i1}^2 + l_{i2}^2 + \cdots + l_{im}^2 \tag{14}$$

The variance portion ψ_i is called uniqueness or specific variance, $i = 1, 2, ..., p$. Therefore, the variance of Y_i is $\sigma_{ii} = h_i^2 + \psi_i$. Consequently, the covariance is explained through the common variances l_{ij}, while the variance is explained by the common variances and the uniqueness [14,24].

It can be demonstrated that the covariance between the vector of original variables $\boldsymbol{Y}$ and the matrix of factors is equivalent to the factor loadings [24]:

$$Cov(\boldsymbol{Y}, \boldsymbol{F}) = E\left[(\boldsymbol{Y} - \boldsymbol{\mu})\boldsymbol{F}^T\right]$$
$$Cov(\boldsymbol{Y}, \boldsymbol{F}) = E\left[(\boldsymbol{LF} + \boldsymbol{\varepsilon})\boldsymbol{F}^T\right]$$
$$Cov(\boldsymbol{Y}, \boldsymbol{F}) = \boldsymbol{L}E\left(\boldsymbol{FF}^T\right) + E\left(\boldsymbol{\varepsilon}\boldsymbol{F}^T\right)$$

$$Cov(Y,F) = LI + 0$$
$$Cov(Y,F) = L \tag{15}$$

This covariance may also be evaluated considering the i-th variable Y_i and the j-th factor F_j, as in Eq. 16 [13]. As the factor loadings l_{ij} represent the covariance between the variable Y_i and the factor F_j, it can be inferred that the factor represents the variables with the highest loadings. Factor analysis aims to estimate the matrices L, Ψ, and F. As it is desired the covariance or correlation structure among the original variables, the common factors are indispensable since the specific factors do not contribute to the covariance explanation [24].

$$Cov(Y_i,F_j) = E\big[(Y_1 - \mu_1)(F_j - \mu_{F_j})\big]$$
$$Cov(Y_i,F_j) = E\big[(l_{i1}F_1 + l_{i2}F_2 + \cdots + l_{ij}F_j + \cdots + l_{im}F_m + \varepsilon_i)F_j\big]$$
$$Cov(Y_i,F_j) = E(l_{i1}F_1F_j + l_{i2}F_2F_j + \cdots + l_{ij}F_jF_j + \cdots + l_{im}F_mF_j + \varepsilon_iF_j)$$
$$Cov(Y_i,F_j) = l_{i1}cov(F_1,F_j) + l_{i2}Cov(F_2,F_j) + \cdots + l_{ij}Var(F_j) + \cdots + l_{im}Cov(F_m,F_j) + Cov(\varepsilon_i,F_j)$$

$$Cov(Y_i,F_j) = l_{i1} \times 0 + l_{i2} \times 0 + \cdots + l_{ij} \times 1 + \cdots + l_{im} \times 0 + 0$$
$$Cov(Y_i,F_j) = l_{ij} \tag{16}$$

In the case of consideration of standardized variables with the associated correlation matrix ρ, the factor model may be expressed according to the Eq. 17 in matrix notation or explicitly through Eq. 18. In this case, the standardized variances are unitary, i.e., $h_i^2 + \psi_i = 1$ [24].

$$\rho = LL^T + \Psi \tag{17}$$

or

$$Var(Y_i) = 1 = l_{i1}^2 + l_{i2}^2 + \cdots + l_{im}^2 + \psi_i$$
$$Cov(Y_i,Y_k) = \rho_{ik} = l_{i1}l_{k1} + l_{i2}l_{k2} + \cdots + l_{im}l_{km} \tag{18}$$

It is possible to get distinct solutions for the same covariance (or correlation) matrix. The non-singularity of the estimated parameters through factor analysis may be used to get a better interpretation of the factors applying distinct rotating methods. Let the orthogonal matrix T, so that $T^TT = I$. The model in Eq. 8 may be rewritten according to Eq. 19, with $L^* = LT$ and $F^* = T^TF$. The new parameters L^* and F^* reproduce the covariance (or correlation) matrix Σ (or ρ) the same way that L and F, for a chosen T rotation matrix aiming to facilitate the interpretation of the factors. It is important to emphasize that the rotation is performed in factors' space [13,14,24].

There are several methods to estimate the parameters of the factor model. Some of the most applied methods are the maximum likelihood, the principal components method and the principal axis (or factor) method. The maximum likelihood method assumes multivariate normality of the data. The principal component method is the simplest method for factor extraction, however, in this method, the covariance matrix $\boldsymbol{\Sigma}$ is not accurately estimated. The variances, $\sigma_{ii} = \sum_{j=1}^{m} l_{ij}^2 + \psi_i = h_i^2 + \psi_i$, are integrally estimated, but the covariances, $\sigma_{ik} = \sum_{j=1}^{m} l_{ij} l_{kj}$, are approximated. The principal component is used to achieve an initial factor solution and may be applied when the covariance matrix is singular. The principal axis method considers an initial estimate of $\boldsymbol{\Psi}$ which is disregarded in the principal component method. The estimation may be performed even if when the covariance (or correlation) matrix is not of full rank [13,14,24].

For these reasons the principal axis method is considered an interesting choice for factor extraction and is elucidated in Appendix A. To achieve a simple structure, with easy to interpret factor-variable relationship, the quartimax, and varimax rotation may be applied. These methods are detailed in Appendix B.

3.1 Data adequacy for factor analysis

The sphericity test of Bartlett [30] tests if the correlation matrix is different from an identity matrix. If the null hypothesis $H_0: \boldsymbol{\Sigma} = \boldsymbol{I}\sigma^2$ is not rejected the variables are not related and unsuitable to be described in terms of few implicit and unobservable quantities called factors. The test is called sphericity test since under H_0 the ellipsoid $(\boldsymbol{y} - \boldsymbol{\mu})^{\mathbf{T}} \boldsymbol{\Sigma}^{-1} (\boldsymbol{y} - \boldsymbol{\mu}) = c^2$ is reduced to a sphere $(\boldsymbol{y} - \boldsymbol{\mu})^{\mathbf{T}} (\boldsymbol{y} - \boldsymbol{\mu}) = \sigma^2 c^2$ [13]. The test statistics considering the sample correlation matrix $\boldsymbol{R}$ is presented in Eq. 19, with $p(p-1)/2$ degrees of freedom, where $|\boldsymbol{R}|$ is the determinant of $\boldsymbol{R}$ [30].

$$\chi_0^2 = -\left[n - (2p + 5)/6\right] \times ln|\boldsymbol{R}| \tag{19}$$

Before performing the factor analysis, it is important to determinate the suitable number of factors. The parallel analysis, Horn [31], plots the ordered eigenvalues as a function of the extracted factors. This analysis compares the eigenvalues of the sample covariance matrix of the variables under study with the eigenvalues of a simulated data matrix. The number of factors to be extracted according to this procedure must be defined as the abscissa point where the two curves intersect. If this point is not an integer it should be considered the closest smaller integer. The scree test [32] is one of the most popular tests. As the parallel analysis, the scree test is a graphical procedure which

also plots the eigenvalues as a function of the extracted factors successively. In this procedure, the number of factors is chosen in the curved part of the plot, considering the factors which contribute most to the explanation of the variability of the data, discarding the factors in the linear part of the plot, which is called scree. Revelle [33] states, the scree test may be appealing, but leave questions as to the breaking point. Parallel analysis, since it contains a simulated curve for comparison, would leave no doubt in the decision.

4   PROPOSED METHOD: MULTIVARIATE GR&R-FA

The proposed multivariate GR&G method through factor analysis is denominated GR&R-FA. The GR&R-FA is proposed to deal with measurement results of distinct variables of interest, which can be separated in few groups with highly correlated variables inside the groups and moderate or no significant correlation between variables of different groups. This data pattern when analyzed with other multivariate GR&R methods such as GR&R-PCA [11], and GR&R-WPC [12], may present inconsistent results, due to the difficulty on the interpretation of the association among the original variables and the transformed variables. As PCA focuses on the interpretation of variances, while factor analysis is designated to account the covariances or correlations, the latter may be more suitable in these cases. Therefore, the GR&R-FA allows the dimensionality reduction with simple to interpret association between original and latent variables, as advocated by Thurstone [34].

The steps to perform the multivariate GR&R-FA method may be followed in the flow chart in Fig. 2 and are depicted as follows:

Step 1: Define the measurement systems, measurement procedure, GR&R design and variables to be measured.

Step 2: Perform the measurements following the GR&R design and store the results.

Step 3: Calculate the sample Pearson correlation between the variables. Define the correlation matrix and test the significance of each correlation.

Step 4: Evaluate if there are significant correlations. If the correlations are not significant univariate GR&R may be performed to each variable separately. If there are significant correlations, a multivariate strategy should be performed to guarantee redundancy decrease and to account the correlation between variables. In this case, proceed to step 5.
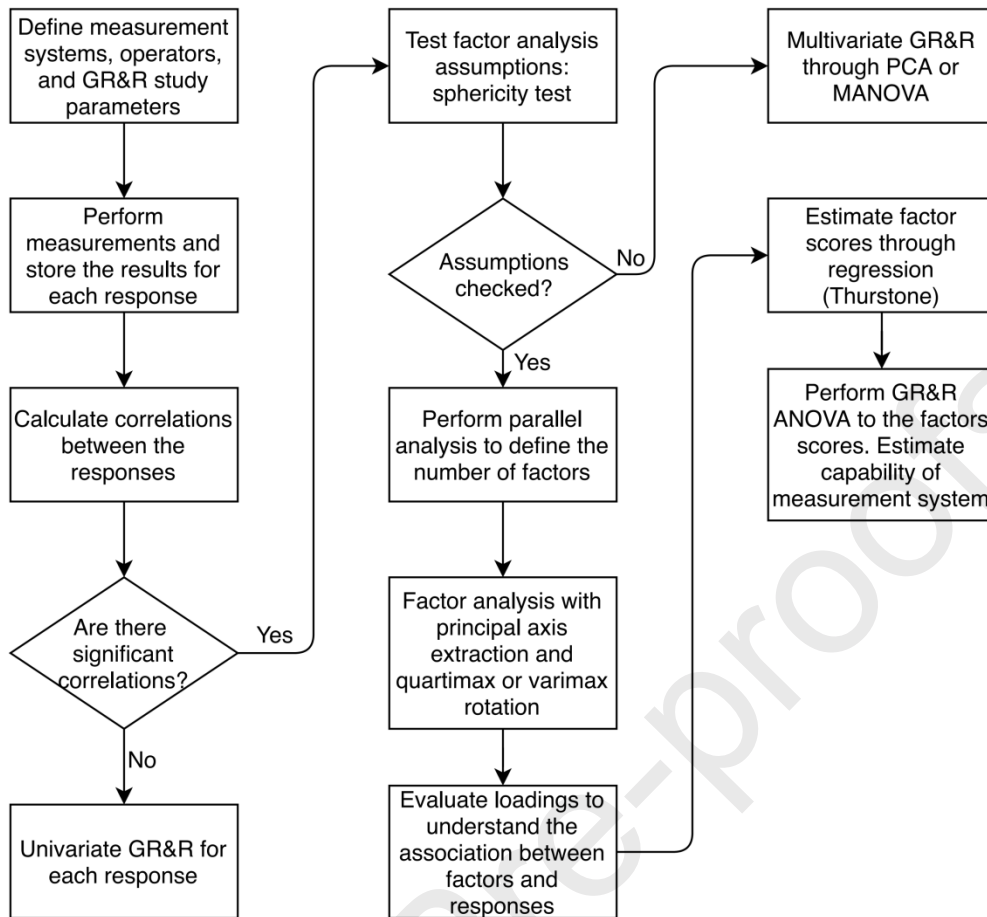
Fig. 2. Flowchart for the GR&R-FA method

Step 5: Test factor analysis assumptions. In this step, the sphericity test is performed to guarantee adequacy for factor analysis.

Step 6: Evaluate the results of the assumptions tests. If the assumptions are not checked, the factor analysis will not generate good results and another multivariate GR&R method may be employed, such as PCA or MANOVA. In the case of assumptions fulfillment, the GR&R-FA flow may be carried on.

Step 7: Define the number of factors to be extracted through the parallel analysis.

Step 8: Perform the factor analysis with the principal axis extraction method with the number of factors defined in step 7. Test the varimax and quartimax rotation methods and compare the results in terms of loadings with the simplest interpretation and highest variance proportion explained by the extracted factors. The extraction and rotation methods are detailed in Appendix A and B, respectively.

Step 9: Estimate the factor scores through regression, as proposed by Thurstone.

Step 10: Perform the GR&R ANOVA to each factor score vector and estimate the capability of the measurement system. The %R&R, *SNR* and *DR* indexes are evaluated to judge the gage capability.

The *PTR* index is not calculated since it is also related to process capability, being out of the scope of the present work. It is essential to highlight that Eqs. 1-10, in section 2, are now applied to scores of factor instead of the original variables (*y*).

5   EXPERIMENTAL APPLICATION

The GR&R-FA study was performed in holes of AISI H13 hardened steel workpieces. The holes were obtained through helical milling process in a CNC machining center ROMI® Discovery 560 with numerical control Siemens® Sinumerik 810D. The end mill used in helical milling tests were ISO/ANSI R215.H4 10050DAC03H 1610 with D_t = 10 mm diameter, z = 4 teeth and $a_{p(máx)}$ = 0.3 mm, Sandvik grade GC 1610, ISO grade H, with $(Ti,Al)N_2$ PVD coating from Sandvik Coromant. Compressed air was applied to put out the chips. Eleven workpieces with distinct hole quality levels were selected, to study the repeatability and reproducibility of the measurement system accounting the entire range of process quality variation. The present MSA study was conducted previously to the modeling and optimization of helical milling of AISI H13 hardened steel study, to guarantee the capability of the measurement system. However, the latter results were published before, see Pereira, et al. [35].

Workpieces of AISI H13 hardened steel were provided by *Proaços®*. This material is recommended for applications in aluminum extrusion dies, and molds for thermoplastics. The cylindrical workpieces were with 24 mm of diameter and 20 mm of height. Holes were obtained in AISI H13 hardened steel workpieces through the helical milling process. All through-holes were obtained with a diameter of 18 mm. Fig. 3 shows the experimental setup.
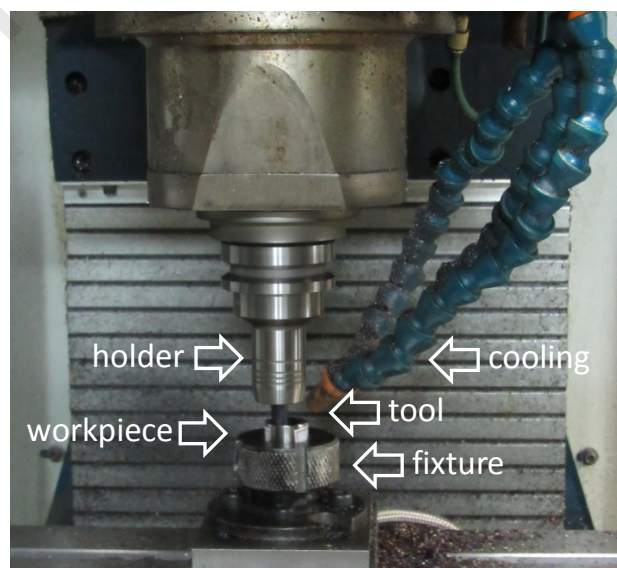

Fig. 3. Experimental setup for the helical milling tests

Microgeometrical and geometrical quality characteristics were measured in the GR&R study. Microgeometrical deviations are commonly called surface roughness. The surface roughness may affect lubrication, friction and corrosion resistance of the surface [36]. Therefore, it is an important quality parameter to indicate the condition of a finished metal surface, especially in the case of holes. The geometrical deviation may affect the coupling of components and the behavior of the mechanical assembly.

Figure 4 presents the roughness profile terminology, with the sampled roughness profile in green. This roughness profile is obtained after filtering the sampled profile. The roughness profile is defined considering the measured profile, called primary profile, by eliminating the long-wave components defined by the cut-off length λ_c, in blue arrow. The cut-off presents the same length of the sampling length, which is the length used to identify the irregularities of the profile under evaluation. The average line, in red, is the line corresponding to the long-wave profile component suppressed by the profile filter λ_c. Finally, the evaluation length (l_n), in orange arrow, is the length used to establish the profile under evaluation.
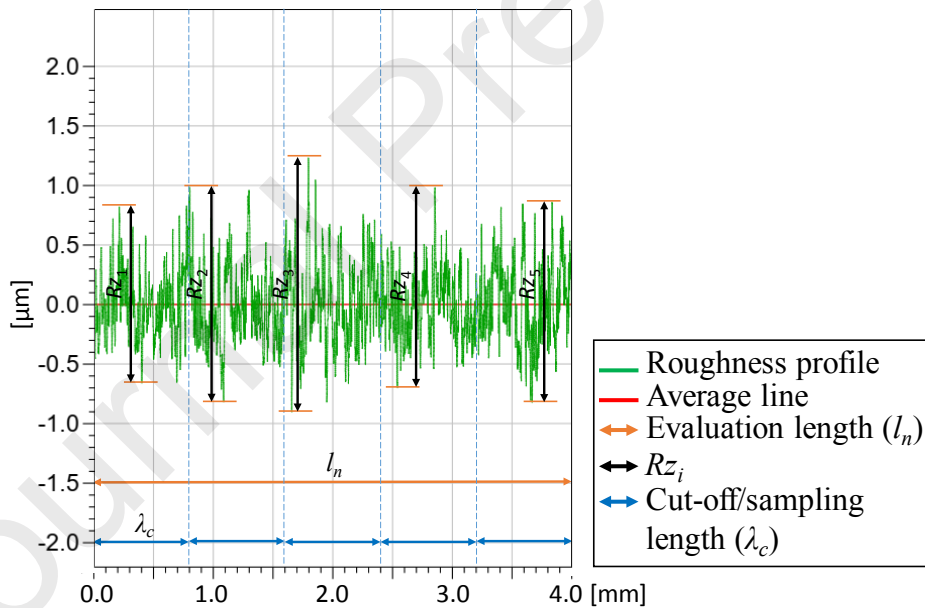
Fig. 4. Roughness measurement terminology

There are several roughness parameters to quantify the sampled surface texture. The main roughness parameter, which is used to define surface texture in mechanical projects, is the average surface roughness, R_a [μm]. R_a is defined as the average of the absolute values of the sampled heights in the evaluation length. Another important roughness parameter is R_q, which is defined as the root mean square average of the profile sampled heights over the evaluation length. These two parameters

may be used as central tendency parameters of the profile. To quantify the dispersion of the profile, the parameter R_z is the average of the amplitude distances Rz_i which are measured in each sampling length, as illustrated in Fig. 4.

Figure 5 shows the roundness and cylindricity terminology, used to quantify the geometrical error in holes and shafts. In the case of a specific transversal section of interest, the roundness measurement may be performed, Fig. 5(a). The roundness sampled profile is represented through a polar plot. In this plot, part of the radial scale is suppressed and the profile is scaled to make the roundness deviations observable. The least-squares circle is calculated considering the deviations of the profile. The sampled profile presents peak and valley deviations, which are respectively the deviations outward and inward concerning the least-squares circle. The radial distance between the least-squares circle and the external circle is called peak roundness (Ron_p). The radial distance between the least-squares circle and the internal circle is called valley roundness (Ron_v). The radial distance between external and internal circles is called total roundness (Ron_t). Consequently, $Ron_t = Ron_p + Ron_v$.
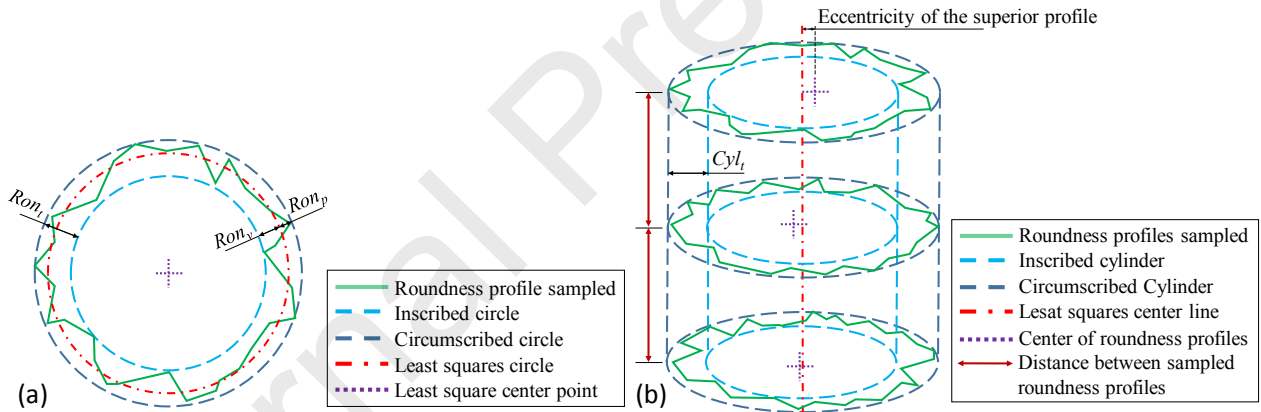
Fig. 5. (a) Roundness measurement; and (b) cylindricity measurement terminology

When the geometrical error is important in all axial height of the cylindrical surface, the cylindricity may be considered. The method of cylindricity measurement used in this work and illustrated in Fig. 5(b) consists in sampling equidistant roundness profiles and in calculating a related cylindricity profile. The center of each roundness profile is calculated through least squares. Taking the center of each roundness profile, a least-squares center line is estimated. Then, an internal and an external cylinder are defined. The radial distance between these cylinders is the total cylindricity, Cyl_t. When measuring the cylindricity through this method, the eccentricity among the profiles is

considered. Consequently, Cyl_t result will be higher than the average Ron_t of the profiles and will account not only the form error but also the position deviation.
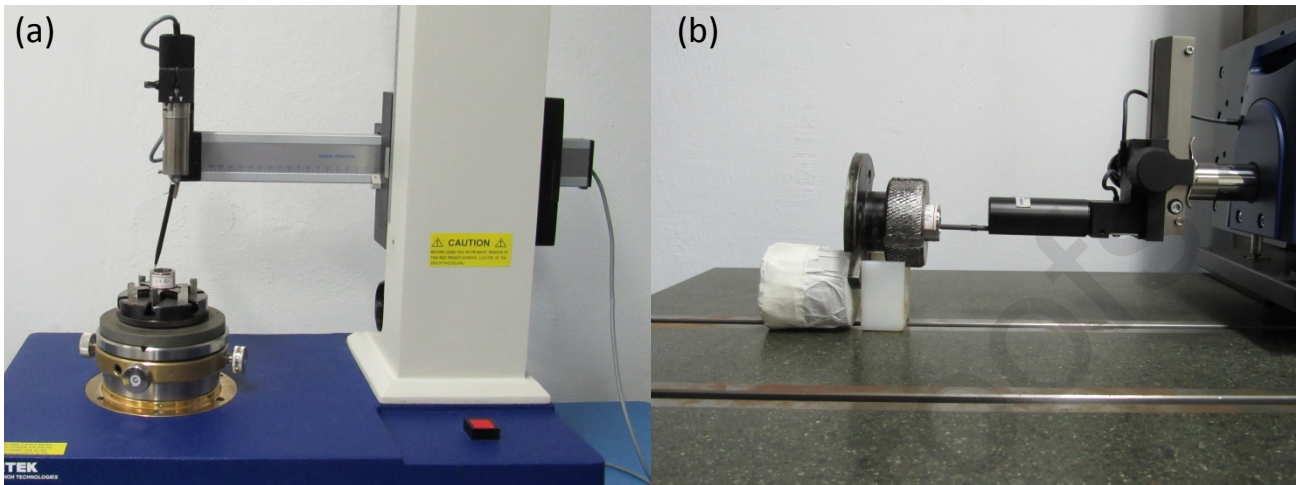

Fig. 6. Setup for (a) roundness; and (b) roughness measurements

The roughness measurements were performed using the roughness and profile measurer *Form Talysurf Intra* from *Taylor Hobson®*. It was considered a cut-off of $\lambda_c = 0.25$ mm. The roundness and cylindricity measurements were obtained through the roundness measurement system *Talyround 131* from *Taylor Hobson®*, with a ruby probe with 2 mm diameter. The applied filter range was 1-50 upr. Fig. 6 illustrates the experimental setup for roundness and roughness measurement. These equipment are both aided by computer and software *ultra* from *Taylor Hobson®*.

The roughness parameters considered in the GR&R study were R_a, R_q, and R_z, while the geometrical error parameters were Ron_p, Ron_t and Cyl_t. The parameter Ron_v was not considered since it can be derived considering Ron_t and Ron_p results. Figure 7 illustrates the positions of the measurements. For roughness, it was considered three positions radially equidistant from 120º, as illustrated in the reference view. The roundness measurement positions were considered in five positions at the end of the hole equidistant of 1.2 mm, as illustrated in section A-A. Generally, the end of the holes obtained through helical milling presents lower quality due to the tool contact and radial force levels, which leads to tool deflection and, consequently, geometrical and microgeometrical deviations. Besides, at the end of the hole, the surface roughness is worst, since the tool peripheral cutting edges pass more times at the beginning of the hole, improving the roughness. It must be stressed that the complete product characterization is necessary for process modeling [35], however, for metrological capability aims, the worst conditions were tested.
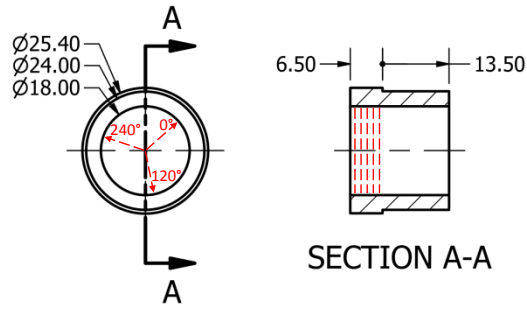
Fig.7. Roundness and roughness measurement positions

The GR&R study was performed considering 3 operators, 11 workpieces and 2 measurements for each operator in each workpiece. Since a GR&R design is a factorial design with random factors, in the present study it was performed $3^1 \times 11^1 \times 2^1 = 66$ measurements in random order. To perform the analysis, it was used the software R [37], aided by the following packages: psych [38], GPArotation [39], corrplot [40], Hmisc [41], ggplot2 [42], SixSigma [43], lme4 [44] and GGally [45].

6   RESULTS AND DISCUSSION

Table 2 presents the 66 measurement results performed in completely random order for the three operators, in the eleven parts, with two replications, for the GR&R study of three microgeometrical and three geometrical error quality characteristics of holes in AISI H13 hardened steel workpieces. Through these results, the surface and the geometrical form of the boreholes may be characterized to ensure the quality control of the holes.

Figure 8 presents the roundness measurement results for part 1, operator 2, and replica 1, with average results $Ron_t = 7.11$ μm and $Ron_p = 2.68$ μm. The polar plots with a scale division of 5μm show the geometrical profile error. For all 66 measurements presented in Table 2, the lowest and highest results for Ron_p were 2.68 μm and 9.32 μm, while for Ron_t were 6.92 μm and 18.94 μm. Considering the five positions of the roundness measurements a cylindricity measurement is calculated by the software. For instance, Fig. 9 presents the cylindricity result for part 2, operator 3, and replica 1, with $Cyl_t = 11.93$ μm. For all 66 measurements, the lowest and highest Cyl_t results were 8.34 μm and 22.96 μm, respectively. These geometrical error results assure promising hole quality. However, it should be evaluated the quality of these measurements guaranteeing low R&R error before using these results for quality control.

Figure 10 presents the roughness measurement results for the part 3, operator 1 and replica 1, with average results of the three radial positions $R_a = 0.23$ μm, $R_q = 0.29$ μm, and $R_z = 1.41$ μm.

Taking all roughness measurements, the lowest and highest results were 0.19 and 0.50 μm for R_a, 1.22 and 2.73 μm for R_z, and 0.24 and 0.61 μm for R_q, respectively.

Table 2. Measurements for GR&R study, all results in [μm]

Parts	Operator	Replica 1						Replica 2					
		Ron_p	Ron_t	Cyl_t	R_a	R_z	R_q	Ron_p	Ron_t	Cyl_t	R_a	R_z	R_q
1	1	3.55	8.33	9.96	0.30	1.76	0.38	3.18	7.80	11.00	0.26	1.59	0.33
1	2	2.68	7.11	10.34	0.29	1.72	0.36	2.72	7.38	9.31	0.30	1.78	0.37
1	3	3.16	7.65	9.76	0.30	1.76	0.38	3.02	7.49	10.57	0.28	1.66	0.35
2	1	5.97	11.25	12.43	0.28	1.66	0.35	6.13	11.50	13.64	0.28	1.66	0.35
2	2	6.43	12.09	14.01	0.27	1.62	0.34	5.51	10.40	11.88	0.27	1.66	0.35
2	3	5.67	10.54	11.93	0.26	1.63	0.34	5.65	10.47	11.85	0.25	1.69	0.35
3	1	6.38	14.53	21.12	0.23	1.41	0.29	6.47	14.80	21.05	0.25	1.49	0.32
3	2	6.86	15.62	21.69	0.24	1.52	0.32	6.71	15.22	20.68	0.25	1.53	0.32
3	3	6.77	15.39	21.22	0.24	1.36	0.29	6.57	15.16	20.28	0.22	1.43	0.30
4	1	3.52	6.94	8.34	0.22	1.32	0.27	3.65	7.44	9.15	0.25	1.46	0.31
4	2	3.52	7.04	8.68	0.24	1.45	0.30	3.55	7.00	8.63	0.21	1.31	0.27
4	3	3.38	6.92	8.71	0.23	1.37	0.29	3.35	6.84	9.02	0.25	1.46	0.31
5	1	5.30	10.02	11.48	0.24	1.42	0.30	5.45	10.02	11.17	0.24	1.42	0.30
5	2	5.18	9.61	11.99	0.25	1.45	0.31	4.98	9.11	10.84	0.24	1.47	0.31
5	3	5.30	9.86	10.94	0.26	1.50	0.32	5.41	10.04	11.09	0.23	1.39	0.29
6	1	3.78	8.16	12.51	0.28	1.76	0.41	3.76	8.16	11.47	0.34	1.87	0.43
6	2	3.73	8.11	12.43	0.32	1.76	0.42	3.83	8.27	13.01	0.33	1.85	0.43
6	3	3.80	8.15	12.57	0.34	1.93	0.46	3.85	8.31	11.18	0.35	1.93	0.46
7	1	6.37	10.86	15.07	0.20	1.28	0.25	6.47	11.19	14.19	0.19	1.23	0.24
7	2	5.71	10.29	12.34	0.20	1.27	0.25	6.37	10.89	13.07	0.20	1.22	0.25
7	3	6.32	10.83	14.55	0.20	1.26	0.25	6.69	11.49	14.57	0.20	1.29	0.25
8	1	5.28	11.36	13.04	0.47	2.68	0.59	4.71	10.49	12.37	0.48	2.72	0.60
8	2	5.10	11.25	13.42	0.47	2.60	0.58	5.11	11.29	12.99	0.49	2.71	0.60
8	3	4.50	9.56	11.27	0.49	2.73	0.61	4.67	10.24	11.77	0.50	2.69	0.61
9	1	3.01	7.14	9.91	0.22	1.37	0.28	3.12	7.30	9.19	0.24	1.42	0.30
9	2	3.26	7.43	8.45	0.23	1.41	0.29	3.33	7.68	9.07	0.24	1.42	0.31
9	3	3.56	7.98	10.21	0.24	1.43	0.30	3.10	7.24	8.79	0.23	1.36	0.29
10	1	4.03	10.14	16.73	0.30	1.82	0.42	4.19	10.44	16.43	0.34	1.85	0.44
10	2	4.56	10.94	18.21	0.30	1.68	0.38	4.22	10.26	16.47	0.36	1.86	0.44
10	3	4.17	10.33	16.86	0.33	1.82	0.41	4.19	9.96	16.95	0.30	1.72	0.38
11	1	9.00	18.26	22.75	0.22	1.33	0.28	8.61	17.52	21.87	0.22	1.30	0.27
11	2	8.80	18.10	22.60	0.23	1.33	0.29	8.65	17.61	21.82	0.23	1.38	0.29
11	3	9.32	18.94	22.96	0.23	1.36	0.29	8.80	17.94	22.96	0.22	1.32	0.28

Position: P1

Ron_t = 9.12 μm
Ron_p = 3.76 μm

Position: P2

Ron_t = 8.15 μm
Ron_p = 3.05 μm

Position: P3

Ron_t = 6.65 μm
Ron_p = 2.56 μm

Position: P4

Ron_t = 6.01 μm
Ron_p = 2.13 μm

Position: P5

Ron_t = 5.61 μm
Ron_p = 1.91 μm

P1 – P5

SECTION A-A

13

6.50

A   A

Ø25.40
Ø24.00
Ø18.00

Fig. 8. Roundness measurements, part 1, operator 2, and replica 1. Ron_t = 7.11 μm, Ron_p =2.68 μm

2 μm/div.

Z Height (mm)

P5

P4

P3

P2

P1
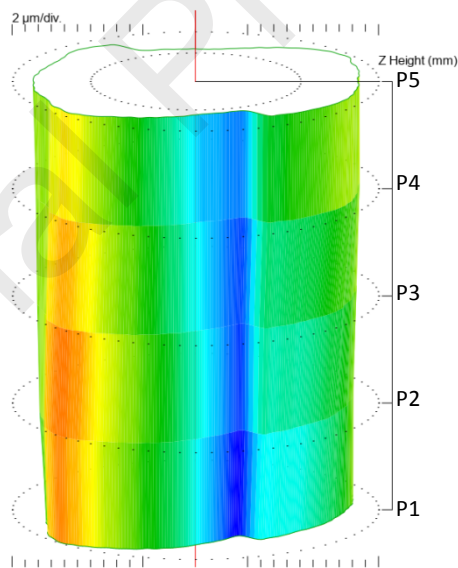
Fig. 9. Cylindricity measurement, part 2, operator 3, and replica 1. Cyl_t = 11.93 μm
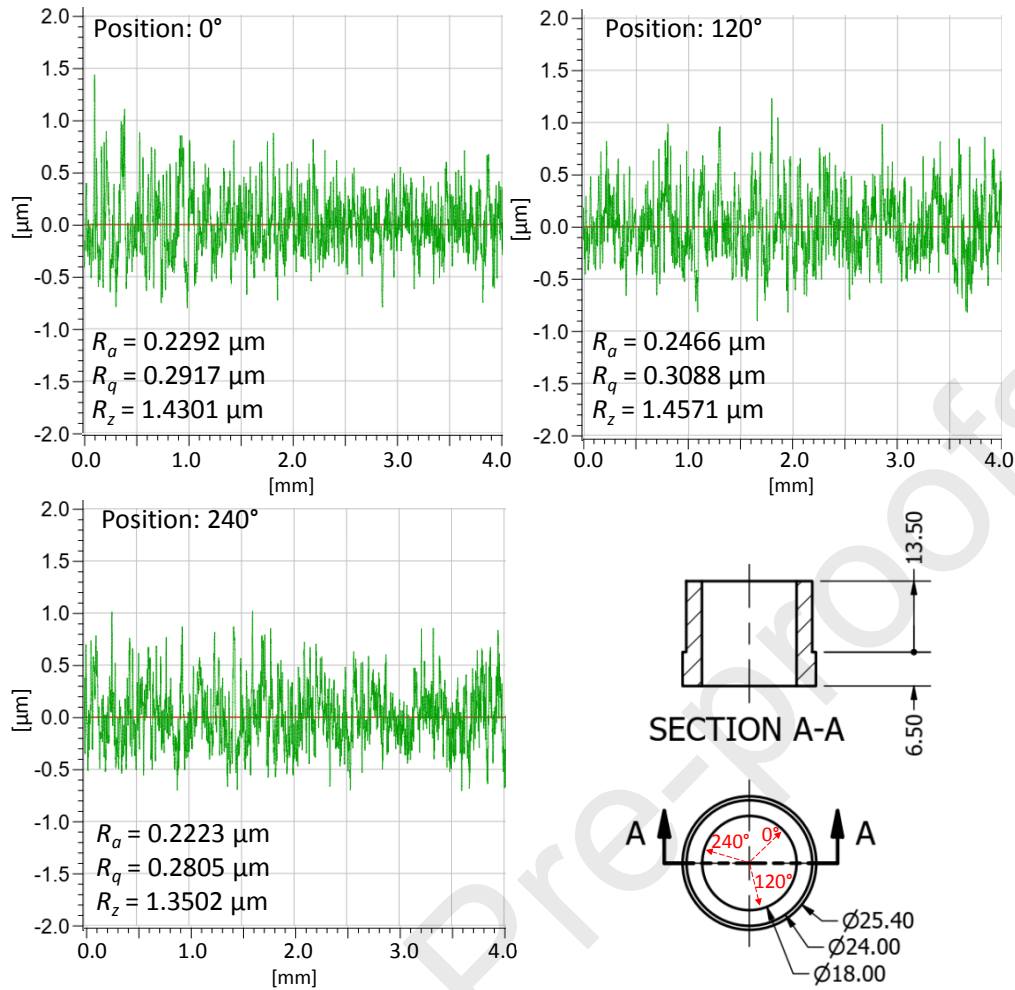
Fig. 10. Roughness measurements, part 3, operator 1, and replica 1. R_a = 0.23 μm, R_q = 0.29 μm, R_z = 1.41 μm;

Before to perform the GR&R study it is necessary to estimate the correlation among the quality variables, considering the covariance among the variables, besides evaluating the possibility of dimensionality reduction. Figure 11 presents the correlation plot for the variables considered in the GR&R study. In the lower matrix of the correlation plot, it is presented the Pearson correlation coefficient, and in the upper matrix, the circles represent the magnitude of the correlation. For both circles and Pearson correlation values, the blue color consists of positive correlation, while the red represents the negative correlations. The variables are hierarchically ordered in the plot according to its correlation values. The values and circles with a cross symbol are not statistically significant. The correlation matrix is also presented in Table 3 with person correlation and p-values.
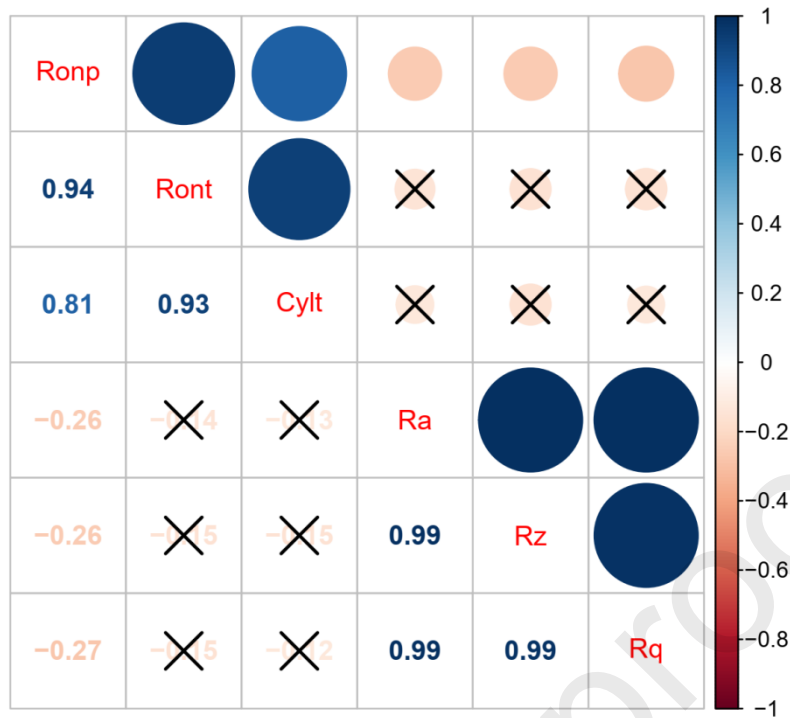
Fig. 11. Correlation plot for the variables of the GR&R study

Table 3. Correlation matrix

	Ron_p	Ron_t	Cyl_t	R_a	R_z
Ron_t	0.944 [a]				
	0.000 [b]				
Cyl_t	0.813	0.932			
	0.000	0.000			
R_a	-0.256	-0.142	-0.127		
	0.038	0.254	0.309		
R_z	-0.257	-0.152	-0.152	0.990	
	0.037	0.224	0.224	0.000	
R_q	-0.274	-0.154	-0.122	0.992	0.990
	0.026	0.216	0.330	0.000	0.000

[a]*Pearson correlation coefficient;* [b]*P-value*

The microgeometrical error variables, R_a, R_q, and R_z are highly correlated among themselves, with 0.99 of correlation in all pairs, forming a group of roughness outcomes. The geometrical error variables are highly correlated among themselves, with the pair Ron_p and Cyl_t with the lowest correlation equal to 0.81 in this group of geometrical quality outcomes. The correlation among the roughness and the geometrical error variables are moderate and negative, with statistical significance only in Ron_p with each one of the roughness variables. This negative moderate correlation can be explained due to the helical milling process parameters. When the feed in the axial direction is lower in contrast with high feed in the peripheral cut, the roughness is improved with quality loss in

roundness, since these parameters are measured in axial and radial directions of the hole, respectively.

As an effort to achieve dimensionality reduction together with simple structure and easy interpretation of the transformed variables, the factor analysis may be performed. Firstly, it is performed Bartlett's sphericity test to assure that the correlation matrix is not an identity matrix. For the correlation matrix presented in Fig. 11 and Table 3, the Bartlett test results in $\chi^2 = 850.82$, with an associated null p-value and 15 degrees of freedom. Therefore, the null hypothesis $H_0: \mathbf{\Sigma} = \mathbf{I}\sigma^2$ is rejected, assuring significant association among the variables.

Subsequently, the parallel analysis is performed to determine the number of factors to extract. Figure 12 shows the parallel analysis considering the principal axis extraction method. As the curves intersect before three factors in the abscissa, it is suggested two factors to be extracted.
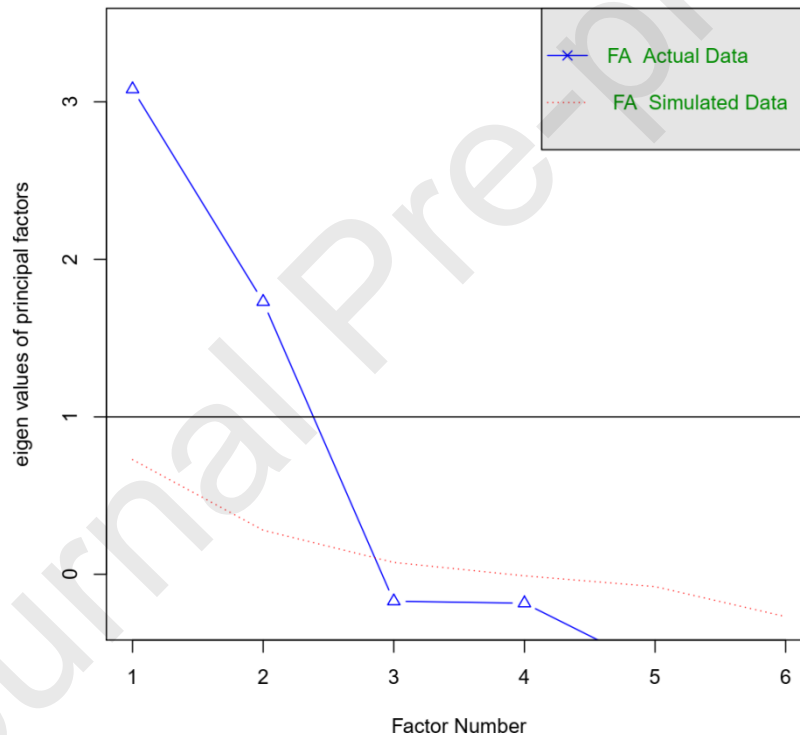

Fig. 12. Parallel analysis for principal axis extraction factor analysis

Table 4 summarizes the factor analysis for the variables Ron_p, Ron_t, Cyl_t, R_a, R_z, R_q considering the correlation matrix, two factors, with the principal axis extraction method and the quartimax rotation. With this extraction and rotation methods, it was achieved a simple structure. In the appendix, it presented the varimax rotation results which presented a bit lower cumulative proportion of the variance explained by the factors when compared to the quartimax rotation. Through quartimax rotation, the first axis (PA_1) is highly correlated with the variables R_a, R_z, and R_q,

with all loadings equal to 0.99. The second axis is highly correlated with the variables Ron_p, Ron_t and Cyl_t, with loadings 0.93, 0.99 and 0.94, respectively. The quartimax rotation provides this pattern by maximizing the variance among the factors. Therefore, PA_1 is a roughness axis and PA_2 is a roundness axis, as demonstrated in the factor analysis diagram in Fig. 13. It is important to note that the factor PA_1, which is related to roughness, presented a loading of -0.19 with the variable Ron_p, due to the moderate negative correlation between this variable and the roughness outcomes. However, the extracted factors are independent, as quartimax is an orthogonal rotation method.

Table 4. Factor analysis results, with principal axis extraction method and quartimax rotation

	PA_1	PA_2	h_i^2	ψ_i	$Var(Y_i)$
Ron_p	-0.19	0.93	0.89	0.11	1.0
Ron_t	-0.07	0.99	0.99	0.01	1.0
Cyl_t	-0.05	0.94	0.88	0.12	1.0
R_a	0.99	-0.08	0.99	0.01	1.0
R_z	0.99	-0.09	0.99	0.01	1.0
R_q	0.99	-0.09	0.99	0.01	1.0
$Var(PA_j)$	2.99	2.74			
Proportion Var	0.5	0.46			
Cumulative Var	0.5	0.96			

The common variance h_i^2 describes the variance retained by the factors in each variable, describing the correlation and part of the variance of the i-th variable, while the uniqueness ψ_i retains the remaining part of the variance of the i-th variable. Since the analysis considered the correlation matrix, the variance $Var(Y_i)$ is unitary for all variables. The proportion of the variance explained by the factor PA_1 is 0.5, while the proportion explained by the factor PA_2 is 0.46, totalizing 0.96 of the proportion of data variability explained by the extracted factors.
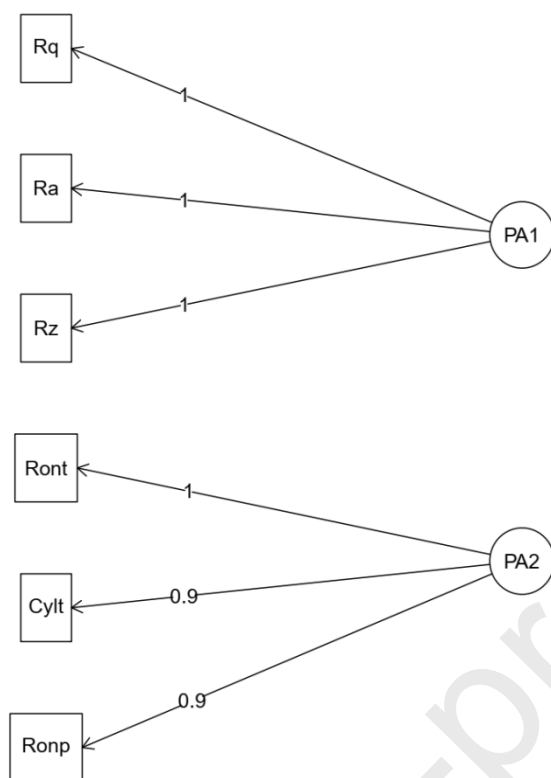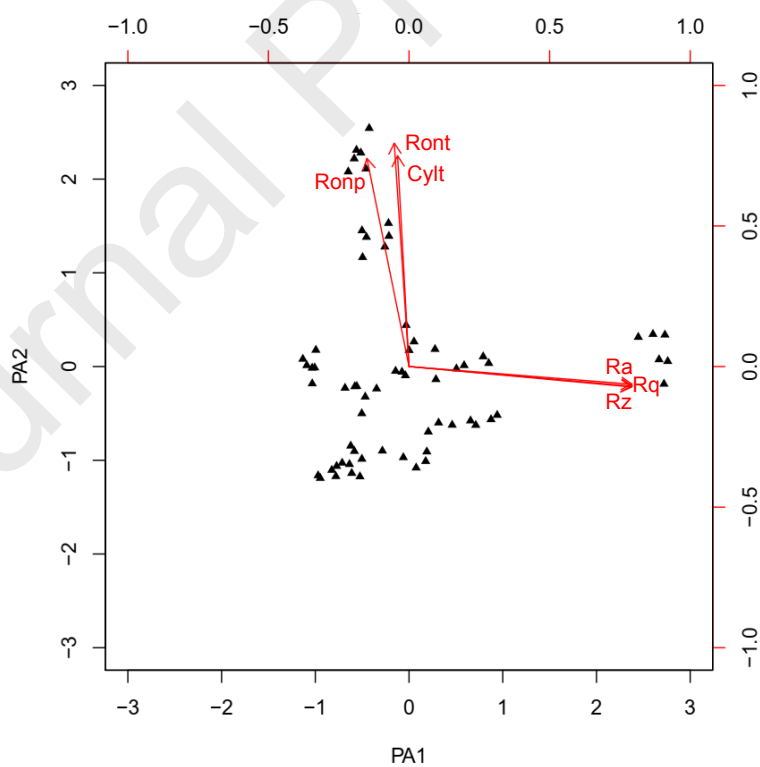
Fig. 13. Factor analysis diagram

Fig. 14. Biplot for principal axis factor analysis with quartimax rotation

The interpretation of the factors is clear since in each factor the loadings are high only for a group of highly correlated variables, making it easy to relate each factor to the related group of variables. Figure 14 illustrates the biplot for the factor analysis through principal axis extraction and quartimax rotation. As can be observed the variables R_a, R_q, and R_z present loadings with expressive coordinates in the direction of the factor PA_1, while the variables Ron_p, Ron_t and Cyl_t presents expressive coordinates in the direction of the factor PA_2.

To perform further analysis with the transformed variables the scores of the two factors are obtained. Table 5 presents the scores for the factors PA_1 and PA_2 estimated by regression with R^2 of 99.82% and 99.60%, respectively.

Table 5. Scores of the factors PA_1 and PA_2

Parts	Operator	Replica 1		Replica 2		Parts	Operator	Replica 1		Replica 2	
		PA_1	PA_2	PA_1	PA_2			PA_1	PA_2	PA_1	PA_2
1	1	0.205	-0.700	-0.285	-0.904	7	1	-1.009	-0.012	-1.135	0.080
1	2	0.078	-1.063	0.177	-1.016	7	2	-1.035	-0.183	-1.093	0.012
1	3	0.189	-0.913	-0.061	-0.975	7	3	-1.036	-0.016	-0.996	0.176
2	1	0.001	0.174	0.053	0.266	8	1	2.607	0.347	2.672	0.076
2	2	-0.031	0.443	-0.039	-0.096	8	2	2.450	0.316	2.735	0.340
2	3	-0.144	-0.048	-0.076	-0.058	8	3	2.725	-0.186	2.765	0.057
3	1	-0.496	1.170	-0.258	1.283	9	1	-0.826	-1.111	-0.637	-1.048
3	2	-0.219	1.536	-0.215	1.397	9	2	-0.715	-1.034	-0.584	-0.908
3	3	-0.502	1.457	-0.455	1.386	9	3	-0.624	-0.851	-0.775	-1.068
4	1	-0.949	-1.197	-0.505	-0.992	10	1	0.507	-0.023	0.793	0.107
4	2	-0.613	-1.144	-0.972	-1.169	10	2	0.278	0.186	0.852	0.036
4	3	-0.783	-1.177	-0.525	-1.180	10	3	0.589	0.012	0.287	-0.138
5	1	-0.559	-0.211	-0.580	-0.214	11	1	-0.561	2.319	-0.649	2.088
5	2	-0.468	-0.325	-0.506	-0.504	11	2	-0.514	2.290	-0.460	2.119
5	3	-0.347	-0.238	-0.684	-0.231	11	3	-0.425	2.554	-0.585	2.227
6	1	0.316	-0.602	0.713	-0.628						
6	2	0.461	-0.626	0.657	-0.580						
6	3	0.876	-0.566	0.942	-0.520						

After dealing with the correlation structure, describing the variables in two non-observable and orthogonal factors through principal axis factor analysis with quartimax rotation, the GR&R analysis is performed. Table 6 summarizes the GR&R analysis for the roughness factor PA_1 and the roundness factor PA_2. The interactions are removed, considering the significance value α = 0.05, for both factors PA_1 and PA_2. The ANOVA indicates statistical significance only for the Parts, with evidence of rejection of the null hypothesis of equality of the Parts. The Operators present homogeneity in the measurements concerning roughness results, PA_1, and about roundness, PA_2.

Table 6. GR&R ANOVA

GR&R ANOVA for PA_1					
	Df	Sum Sq	Mean Sq	F-value	p-value
Parts	10	63.67	6.367	257.847	<2e-16
Operators	2	0.02	0.012	0.475	0.625
Repeatability	53	1.31	0.025		
Total	65	65.00			
GR&R ANOVA for PA_2					
	Df	Sum Sq	Mean Sq	F-value	p-value
Parts	10	63.94	6.394	321.498	<2e-16
Operators	2	0.01	0.004	0.181	0.835
Repeatability	53	1.05	0.020		
Total	65	65.00			

Figure 15 presents the interaction plots for the roughness and roundness factors, PA_1 and PA_2, respectively. A confidence interval bar with $\gamma = 0.95$ considering the repeatability of the measurements is represented in each mean point. As can be observed, the parts are chosen with different levels of roughness and roundness results. By observing only PA_2 results, it can be inferred that there are some parts with redundant results, for example, P7 and P8 with similar geometrical error levels. However, concerning roughness, P7 presents low roughness, while P8 presents high roughness. Some parts with low roughness may present high roundness [35]. The plots confirm the homogeneity among operators, for both factors PA_1 and PA_2, since for each part all means are close and the confidence intervals intersect.

Table 7 summarizes the variance components of the GR&R study for PA_1 and PA_2. For the factor PA_1 the repeatability is the main responsible for the R&R variation which totals 15.11%. For the factor PA_2 the repeatability is also responsible for all R&R variation with 13.56%. For roughness and roundness results the measurement systems are marginal, considering the AIAG criteria illustrated in Fig. 1. As the reproducibility was negligible, the main problem for both measurement systems are related not to the operators, but the instruments. This natural variation or the random error when a single operator measures the same item successively in a short time is called repeatability. Taking PA_1 and PA_2, which are related to roughness and roundness, respectively, and therefore were measured through different measurement systems, both may be classified as marginal according to the AIAG criteria illustrated in Fig. 1. The obtained capability levels were considered satisfactory for the helical milling hole quality characterization.
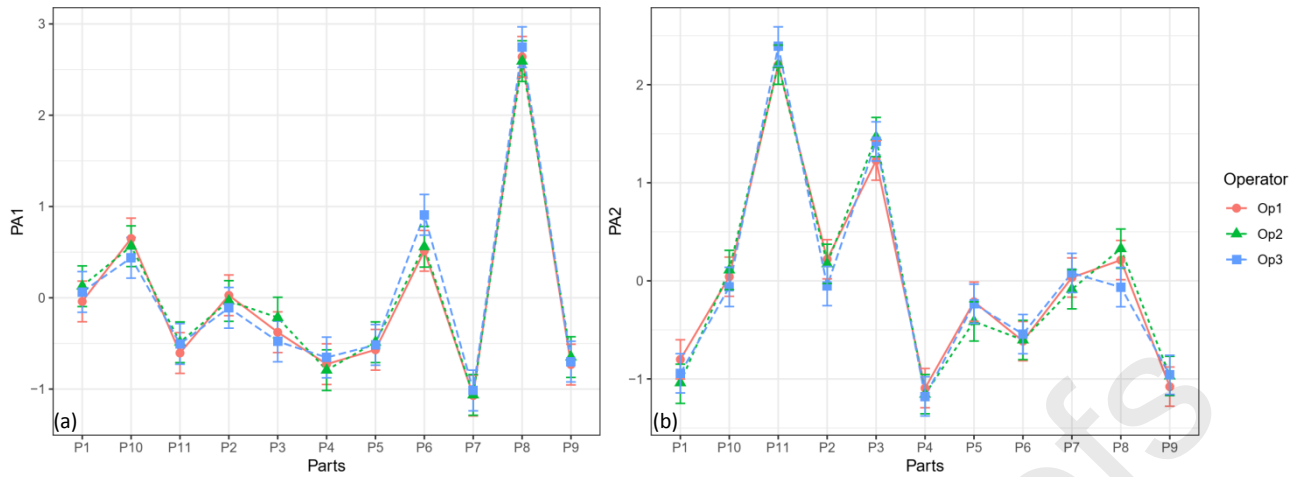
Fig. 15. Interaction plot for (a) PA_1; and (b) PA_2

Table 7. Variance components contribution

Contribution for PA_1			
	StdDev	StudyVar	%StudyVar
Total R%R	0.157	0.943	15.11
Repeatability	0.157	0.943	15.11
Reproducibility	0.000	0.000	0.00
Operators	0.000	0.000	0.00
Part-To-Part	1.028	6.169	98.85
Total	1.040	6.240	100.00
Contribution for PA_2			
	StdDev	StudyVar	%StudyVar
Total R%R	0.141	0.846	13.56
Repeatability	0.141	0.846	13.56
Reproducibility	0.000	0.000	0.00
Operators	0.000	0.000	0.00
Part-To-Part	1.031	6.184	99.08
Total	1.040	6.242	100.00

The *SNR* and *DR* indexes are also important to quantify the gage capability. Table 8 summarizes these measures for PA_1 and PA_2. For both factors the results of *SNR* and *DR* are greater than four, assuring the gage capability for measuring roughness and roundness.

Table 8. Gage capability indexes

Index	PA_1	PA_2
SNR(ndc)	9	10
DR	9.31	10.38

To give a final outlook, Fig. 16 presents a correlation plot for the two factors, with density plots and box plots to see the distributions of the measurements for the distinct operators. The

correlation for PA_1 and PA_2 within each operator is nearby zero, confirming the orthogonality of the factors obtained by factor analysis with principal axis extraction and quartimax rotation. Through density plots and boxplots, it can be visualized the homogeneity among operators. The density plots also show the distribution of the part variability, showing asymmetry of the hole quality variability due to the random selection of the parts for the R&R study. The proposed GR&R-FA method is a distribution-free approach for multivariate GR&R since FA through principal axis extraction do not require a specific probability distribution.
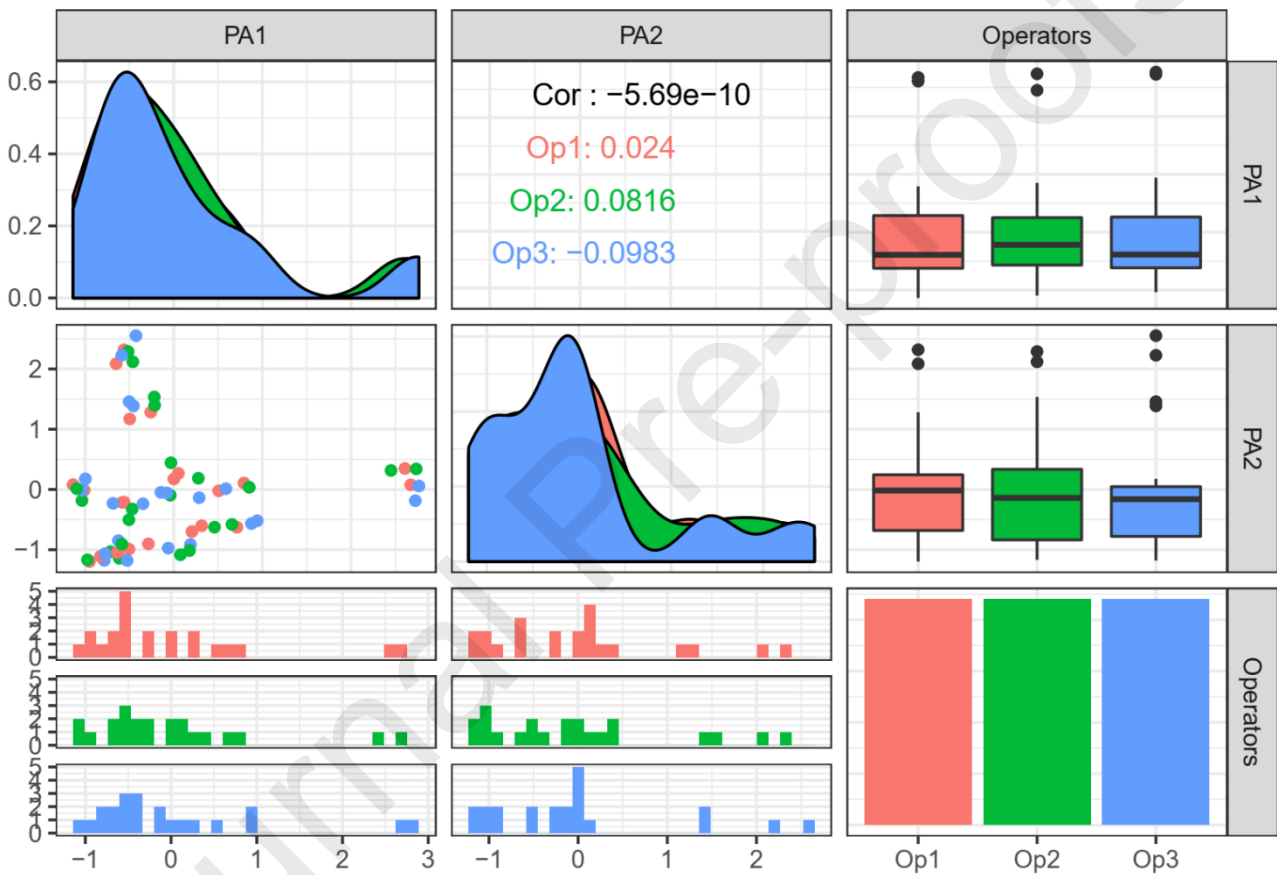

Fig. 16. Final outlook for the GR&R-FA method applied to the helical milling hole quality characterization

7 CONCLUSIONS

This paper presents a multivariate GR&R method through factor analysis. The methodology was applied in the quality evaluation of holes obtained through helical milling in AISI H13 hardened steel. The proposed GR&R-FA method can also be applied in other multivariate GR&R tasks.

Holes obtained through helical milling process in AISI H13 hardened steel parts were evaluated considering roughness, roundness and cylindricity parameters. The roughness parameters

were R_a, R_q, and R_z, the roundness parameters were R_t and R_p, and the cylindricity parameter was Cyl_t. These variables measure distinct microgeometrical and geometrical characteristics and should be considered for a suitable evaluation of the hole quality.

The correlation structure of the variables pointed out high correlations between the roughness variables and high correlations between the roundness variables, with moderate correlation between the variables of these two groups.

The sphericity test was performed assuring adequacy of the correlation matrix for factor analysis. The parallel analysis suggested the extraction of two factors. Factor analysis through principal extraction method and quartimax rotation was applied and the variables were separated into two factors, PA_1 with high loadings related to roughness variables and PA_2 with high loadings related to roundness variables.

GR&R ANOVA was performed in the factor scores of PA_1 and PA_2 obtained through regression. For the factor PA_1, related to roughness, the repeatability was the main responsible for the R&R variation which totals 15.11%. For the factor PA_2, related to roundness, the repeatability was also responsible for all R&R variation with 13.56%. For roughness and roundness results the measurement systems were marginal, considering the AIAG criteria.

The results assure that for some multivariate cases with variables separated into distinct groups with high correlation between variables of the same group and moderate correlation between variables of distinct groups the GR&R-FA is a suitable multivariate GR&R approach.

Some procedures were beyond the scope of the present study. Therefore, limitations may be pointed out. Factor extraction is possible through different methods and rotations. This study focused on the factor analysis performed only through the principal axis extraction method and the varimax and quartimax rotation methods. Thus, in future studies, the GR&R-FA method may be addressed considering distinct rotation and extraction methods and their comparisons. Furthermore, only three roughness parameters and three geometrical error parameters were considered in this work. In future studies, other parameters for roughness and geometrical error may be explored, as well as other characteristics of the parts, such as hole diameter. Lastly, the results of this work were obtained through a crossed GR&R. Therefore, later the factor analysis may be applied to destructive studies (nested GR&R) or studies involving additional sources of variability, such as distinct measurement systems (expanded GR&R).

ACKNOWLEDGEMENTS

REFERENCES

[1]   R.S. Peruchi, P. Rotela Junior, T.G. Brito, J.J.J. Largo, P.P. Balestrassi, Multivariate process capability analysis applied to AISI 52100 hardened steel turning, Int. J. Adv. Manuf. Technol. 95 (2018) 3513–3522. doi:10.1007/s00170-017-1458-8.

[2]   R.S. Peruchi, A.P. Paiva, P.P. Balestrassi, J.R. Ferreira, R. Sawhney, Weighted approach for multivariate analysis of variance in measurement system analysis, Precis. Eng. 38 (2014) 651–658. doi:10.1016/j.precisioneng.2014.03.001.

[3]   P. Veiga, L. Mendes, L. Lourenço, A retrospective view of statistical quality control research and identification of emerging trends: a bibliometric analysis, Qual. Quant. 50 (2015) 673–692. doi:10.1007/s11135-015-0170-8.

[4]   K.D. Majeske, Approval Criteria for Multivariate Measurement Systems, J. Qual. Technol. 40 (2008) 140–153.

[5]   R.S. Peruchi, P.P. Balestrassi, A.P. De Paiva, J.R. Ferreira, M. De Santana Carmelossi, A new multivariate gage R&R method for correlated characteristics, Int. J. Prod. Econ. 144 (2013) 301–315. doi:10.1016/j.ijpe.2013.02.018.

[6]   R.S. Peruchi, H.J. Junior, N.J. Fernandes, P.P. Balestrassi, A.P. de Paiva, Comparisons of multivariate GR&R methods using bootstrap confidence interval, Acta Sci. - Technol. 38 (2016). doi:10.4025/actascitechnol.v38i4.29294.

[7]   AIAG, Measurement systems analysis: reference manual, Fourth ed., Detroit, MI, USA, 2010.

[8]   M.J. Flynn, S. Sarkani, T.A. Mazzuchi, Regression Analysis of Automatic Measurement Systems, 58 (2009) 3373–3379. doi:10.1109/TIM.2009.2025467.

[9]   S.G. He, G.A. Wang, D.F. Cook, Multivariate measurement system analysis in multisite testing: An online technique using principal component analysis, Expert Syst. Appl. 38 (2011) 14602–14608. doi:10.1016/j.eswa.2011.05.022.

[10] F.K. Wang, T.W. Chien, Process-oriented basis representation for a multivariate gauge study, Comput. Ind. Eng. 58 (2010) 143–150. doi:10.1016/j.cie.2009.10.001.

[11] F. Wang, C. Yang, Applying principal component analysis to a GR&R study, J. Chinese Inst. Ind. Eng. 24 (2007) 182–189.

[12] R.S. Peruchi, P.P. Balestrassi, A.P. De Paiva, J.R. Ferreira, M. De Santana Carmelossi, A new multivariate gage R&R method for correlated characteristics, Int. J. Prod. Econ. 144 (2013). doi:10.1016/j.ijpe.2013.02.018.

[13] A.C. Rencher, Methods of multivariate analysis, 2nd ed., John Wiley & Sons, New York, NY, 2002. doi:10.1016/S0378-3758(96)00098-5.

[14] R.A. Johnson, D.W. Wichern, Applied multivariate statistical analysis, 6th ed., Upper Saddle River, NJ, 2007.

[15] R.K. Burdick, C.M. Borror, D.C. Montgomery, Design and analysis of gauge R&R studies: making decisions with confidence intervals in random and mixed ANOVA models, Philadelphia, PA, 2005.

[16] G. Aquila, R.S. Peruchi, P. Rotela Junior, L.C.S. Rocha, A.R. de Queiroz, E. de O. Pamplona, P.P. Balestrassi, Analysis of the wind average speed in different Brazilian states using the nested GR&R measurement system, Meas. J. Int. Meas. Confed. 115 (2018) 217–222. doi:10.1016/j.measurement.2017.10.048.

[17] D.C. Montgomery, Design and Analysis of Experiments, Eighth Ed., John Wiley & Sons, 2013. doi:10.1198/tech.2006.s372.

[18] R.B.D. Pereira, R.S. Peruchi, A.P. De Paiva, S.C. Da Costa, J.R. Ferreira, Combining Scott-Knott and GR&R methods to identify special causes of variation, Meas. J. Int. Meas. Confed. 82 (2016) 135–144. doi:10.1016/j.measurement.2015.12.033.

[19] A. Al-Refaie, N. Bata, Evaluating measurement and process capabilities by GR&R with four quality measures, Meas. J. Int. Meas. Confed. 43 (2010) 842–851. doi:10.1016/j.measurement.2010.02.016.

[20] D.P. Mader, J. Prins, R.E. Lampe, D.P. Mader, J. Prins, R.E. Lampe, The economic impact of measurement error, Qual. Eng. 11 (1999) 563–574. doi:10.1080/08982119908919276.

[21] D.N. Lawley, A.E. Maxwell, Factor Analysis as a Statistical Method, J. R. Stat. Soc. Ser. D (The Stat. 12 (1962) 209–229.

[22] C. Spearman, "General Intelligence," Objectively Determined and Measured, Am. J. Psychol. 15 (1904) 201–293. doi:10.2307/1412107.

[23] L.L. Thurstone, Multiple factor analysis, Psychol. Rev. 38 (1931) 406–427. doi:10.1037/h0069792.

[24] D.F. Ferreira, Estatística multivariada, 2ª edição, UFLA, Lavras, 2011.

[25] J. Liu, J. Shi, S.J. Hu, Engineering-Driven Factor Analysis for Variation Source Identification in Multistage, J. Manuf. Sci. Eng. 130 (2008) 1–10. doi:10.1115/1.2950064.

[26] O. Ha, S. Brown, A factor analysis of Statics Concept Inventory data from practicing civil engineers, in: 2016 IEEE Front. Educ. Conf., 2016: pp. 1–4.

[27] H. Park, S. Kwon, Factor Analysis of Construction Practices for Infrastructure Projects in Korea, KSCE J. Civ. Eng. 15 (2011) 439–445. doi:10.1007/s12205-011-1064-5.

[28] R. Patriarca, J. Bergström, G. Di Gravio, F. Costantino, Resilience engineering: Current status of the research and future challenges, Saf. Sci. 102 (2018) 79–100. doi:10.1016/j.ssci.2017.10.005.

[29] S. Jiahang, W. Jun, H. Side, Annals of Nuclear Energy Identification of unknown spent nuclear fuel with factor analysis for nuclear forensic purpose, Ann. Nucl. Energy. 126 (2019) 43–47. doi:10.1016/j.anucene.2018.10.053.

[30] M.S. Bartlett, The Effect of Standardization on a $\chi 2$ Approximation in Factor Analysis, Biometrika. 38 (1951) 337–344. doi:10.2307/2332580.

[31] J.L. Horn, A rationale and test for the number of factors in factor analysis, Psychometrika. 30 (1965) 179–185.

[32] R.B. Cattell, the Scree Test for the Number, Multivariate Behav. Res. 1:2 (1966) 245–276. doi:10.1207/s15327906mbr0102.

[33] W. Revelle, How to: Use the psych package for factor analysis and data reduction, (2016) 1–86.

[34] L.L. Thurstone, Multiple-factor analysis: a development and expansion of the vectors of mind, 1947.

[35] R.B.D. Pereira, L.A. da Silva, C.H. Lauro, L.C. Brandão, J.R. Ferreira, J.P. Davim, Multi-objective robust design of helical milling hole quality on AISI H13 hardened steel by normalized normal constraint coupled with robust parameter design, Appl. Soft Comput. 75 (2019) 652–685. doi:10.1016/j.asoc.2018.11.040.

[36] R.B.D. Pereira, C.A.A. Hincapie, P.H. da Silva Campos, A.P. de Paiva, J.R. Ferreira, Multivariate global index and multivariate mean square error optimization of AISI 1045 end milling, Int. J. Adv. Manuf. Technol. (2016) 1–15. doi:10.1007/s00170-016-8703-4.

[37] R Core Development Team, R: A Language and Environment for Statistical Computing, Vienna, Austria, 2008. doi:10.1007/978-3-540-74686-7.

[38] W. Revelle, psych: Procedures for Psychological, Psychometric, and Personality Research, (2019). https://personality-project.org/r/psych.

[39] C.A. Bernaards, R.I. Jennrich, Gradient projection algorithms and software for arbitrary rotation criteria in factor analysis, Educ. Psychol. Meas. 65 (2005) 676–696. doi:10.1177/0013164404272507.

[40] T. Wei, V. Simko, R package "corrplot": Visualization of a Correlation Matrix, Statistician. (2017) 1–18.

[41] F.E. Harrell Jr, C. Dupont, Hmisc: Harrell Miscellaneous. R package version 4.2-0, (2019). https://cran.r-project.org/package=Hmisc.

[42] H. Wickham, ggplot2: Elegant Graphics for Data Analysis, New York, 2016. doi:10.1007/978-0-387-98141-3.

[43] A. Cano, Emilio L., M. Moguerza, Javier, Redchuk, Six Sigma with R: Statistical Engineering for Process Improvement, New York, 2012.

[44] D. Bates, M. Mächler, B.M. Bolker, S.C. Walker, Fitting Linear Mixed-Effects Models Using lme4, 67 (2015). doi:10.18637/jss.v067.i01.

[45] B. Schloerke, J. Crowley, D. Cook, H. Hofmann, H. Wickham, F. Briatte, M. Marbach, E. Thoen, A. Elberg, J. Larmarange, GGally: Extension to ggplot2, (2019). https://ggobi.github.io/ggally, https://github.com/ggobi/ggally.

[46] B.J. Neuhaus, C. Wrigley, The quartimax method, Br. J. Stat. Psychol. 7 (1954) 81–91.

[47] H.F. Kaiser, The varimax criterion for analytic rotation in factor analysis, Psychometrika. 23 (1958) 187–200. doi:10.1007/BF02289233.

APPENDIX A. THE PRINCIPAL AXIS EXTRACTION METHOD

In the principal axis an initial estimate $\mathbf{\Psi}_0$ of $\mathbf{\Psi}$ is considered and the spectral theorem is applied to estimate $\boldsymbol{S} - \mathbf{\Psi}$ or $\boldsymbol{R} - \mathbf{\Psi}$, were $\boldsymbol{S}$ is the sample covariance matrix and $\boldsymbol{R}$ is the sample correlation matrix [13]. The method is based in the minimization of the sum of squares of $\boldsymbol{S} - \mathbf{\Sigma}$. Let Q be the sum of squares of the elements of $\boldsymbol{S} - \mathbf{\Sigma}$ exposed in Eq. A.1 [24].

$$Q = tr\left[(\boldsymbol{S} - \mathbf{\Sigma})^2\right] \tag{A.1}$$

Replacing the Eq. 12 in Eq. A.1:

$$Q = tr\left[(\boldsymbol{S} - \boldsymbol{L}\boldsymbol{L}^T - \mathbf{\Psi})^2\right] \tag{A.2}$$

$$Q = tr(\boldsymbol{S}^2) + tr(\boldsymbol{L}\boldsymbol{L}^T\boldsymbol{L}\boldsymbol{L}^T) + tr(\mathbf{\Psi}^2) - 2 \times tr(\boldsymbol{L}\boldsymbol{L}^T\boldsymbol{S}) - 2 \times tr(\boldsymbol{S}\mathbf{\Psi}) + 2 \times tr(\boldsymbol{L}\boldsymbol{L}^T\mathbf{\Psi}) \tag{A.3}$$

The first derivative of Q with regard to L equated to zero results in the Eq. A.4, while the first derivative of Q with regard to Ψ equated to zero results in the Eq. A.5 [24].

$$\frac{\partial Q}{\partial L} = 4LL^T L - 4SL + 4\Psi L = 0$$
$$(S - LL^T - \Psi)L = 0 \tag{A.4}$$

$$\frac{\partial Q}{\partial \Psi} = 2\Psi - 2 \times diag(S) + 2 \times diag(LL^T) = 0$$
$$\Psi = diag(S - LL^T) \tag{A.5}$$

Taking the initial estimate Ψ_0 of Ψ in Eq. A.4, it is obtained the Eq. A.6. By doing $S_r = S - \hat{\Psi}_0$, considering $L^T L$ diagonal, L may be estimated by the spectral decomposition theorem of S_r, i.e., $S_r = \hat{P}\hat{\Lambda}\hat{P}^T$, according to the Eq. A.7 [24].

$$(S - \hat{\Psi}_0)\hat{L} - \hat{L}(\hat{L}^T\hat{L}) = 0$$
$$(S - \hat{\Psi}_0)\hat{L} = \hat{L}(\hat{L}^T\hat{L}) \tag{A.6}$$

$$\hat{L} = \hat{P}\hat{\Lambda}^{1/2} = \left[\sqrt{\hat{\lambda}_1\hat{e}_1} \ \sqrt{\hat{\lambda}_2\hat{e}_2} \ \cdots \ \sqrt{\hat{\lambda}_m\hat{e}_m}\right] \tag{A.7}$$

Therefore, $S_r = S - \hat{\Psi}_0 = LL^T$. If the estimated matrix for Ψ is suitable, S_r will present rank m, i.e., will have all m lines linearly independent and the $p - m$ ignored eigenvalues will be null. However, in practice, the rank of S_r is higher than m, so that the reproduction of S_r is not perfect [24].

The i-th diagonal element of S_r is equal to $s_{ii} - \psi_i$ which consists of the i-th common variance $\hat{h}_i^2 = s_{ii} - \psi_i$. In the case of factorization of the correlation matrix, $R_r = R - \hat{\Psi}_0$, the diagonal element is $\hat{h}_i^2 = 1 - \psi_i$. Therefore, the matrices S_r and R_r are respectively as follows [13]:

$$S_r = \begin{bmatrix} \hat{h}_1^2 & s_{12} & \dots & s_{1p} \\ s_{21} & \hat{h}_2^2 & \cdots & s_{2p} \\ \vdots & \vdots & \ddots & \vdots \\ s_{p1} & s_{p2} & \dots & \hat{h}_p^2 \end{bmatrix} \tag{A.8}$$

$$\boldsymbol{R}_r = \begin{bmatrix} \hat{h}_1^2 & r_{12} & \dots & r_{1p} \\ r_{21} & \hat{h}_2^2 & \dots & r_{2p} \\ \vdots & \vdots & \ddots & \vdots \\ r_{p1} & r_{p2} & \dots & \hat{h}_p^2 \end{bmatrix} \tag{A.9}$$

Popular estimates for the common variances in $\boldsymbol{S}_r$ and $\boldsymbol{R}_r$ are based in the coefficient of multiple correlation R_i^2 among Y_i and the other $p-1$ variables, according to Eqs. A.10 and A.11, respectively, were s^{ii} is the i-th diagonal term of $\boldsymbol{S}^{-1}$ and r^{ii} is the i-th diagonal term of $\boldsymbol{R}^{-1}$ [13]. Therefore, the estimate for the i-th common variance in these equations is $\hat{\psi}_{0_i} = 1/s^{ii}$ and $\hat{\psi}_{0_i} = 1/r^{ii}$, respectively, so that $\hat{\boldsymbol{\Psi}}_0 = [diag(\boldsymbol{S}^{-1})]^{-1}$ and $\hat{\boldsymbol{\Psi}}_0 = [diag(\boldsymbol{R}^{-1})]^{-1}$. After to estimate the factor loadings matrix $\boldsymbol{L}$ one must estimate the diagonal matrix of common variances through Eq. A.5 [24].

$$\hat{h}_i^2 = s_{ii} - \frac{1}{s^{ii}} = s_{ii} R_i^2 \tag{A.10}$$

$$\hat{h}_i^2 = 1 - \frac{1}{r^{ii}} = R_i^2 \tag{A.11}$$

According to Rencher [13] the explanation of the j-th factor is obtained through Eq. A.12, were λ_j is the j-th eigenvalue of $\boldsymbol{S}_r$ and $\boldsymbol{R}_r$. As these matrices will not necessarily be positive semi-defined, some modest eigenvalues may be negative.

$$\begin{cases} Explanation\ of\ j - th\ factor = \dfrac{\sum_{i=1}^p \hat{l}_{ij}^2}{tr(\boldsymbol{S}_r)} = \dfrac{\hat{\lambda}_j}{\sum_{i=1}^p s_{ii} - \psi_i} \\[4mm] Explanation\ of\ j - th\ factor = \dfrac{\sum_{i=1}^p \hat{l}_{ij}^2}{tr(\boldsymbol{R}_r)} = \dfrac{\hat{\lambda}_j}{\sum_{i=1}^p 1 - \psi_i} \end{cases} \tag{A.12}$$

Ferreira [24] contend that Eq. A.12 overestimate the proportion of the explained variance, once the specific variances are not considered, since $\boldsymbol{S}_r = \boldsymbol{S} - \hat{\boldsymbol{\Psi}}_0$ and $\boldsymbol{R}_r = \boldsymbol{R} - \hat{\boldsymbol{\Psi}}_0$. Another problem is regarded to Eq. A.7 due to the impossibility on the calculation of square root of negative eigenvalues. Consequently, Ferreira [24] proposed to use Eq. A.13 to estimate the proportion of the variance explained by the j-th factor of $\boldsymbol{S}$ or $\boldsymbol{R}$.

$$
\begin{cases}
Explanation\ of\ j-th\ factor = \dfrac{\Sigma_{i=1}^{p}\hat{l}_{ij}^{2}}{tr(S)} = \dfrac{\hat{\lambda}_{j}}{\Sigma_{i=1}^{p}s_{ii}} \\[4mm]
Explanation\ of\ j-th\ factor = \dfrac{\Sigma_{i=1}^{p}\hat{l}_{ij}^{2}}{tr(R)} = \dfrac{\hat{\lambda}_{j}}{p}
\end{cases}
\tag{A.13}
$$

APPENDIX B. QUARTIMAX AND VARIMAX ROTATION

As previously explained in section 3, the covariance matrix may be decomposed by rotated factors through an orthogonal matrix T, so that $L^{*} = LT$ e $F^{*} = T^{T}F$. This orthogonal transformation is a rigid rotation of coordinated axes. Geometrically the loadings of the i-th line of L are the coordinates of a point in the factors space corresponding to Y_{i}. The rotation results in the coordinates, i.e., in the loadings with regard to the new axes, however, keep the basic geometrical properties unchanged. If it is possible to find a rotation in which each point is near to an axis, the loadings of that variable, represented by the projection of the point the axis, will be high and low for the remaining factors. The purpose is to find a loading matrix L of trivial interpretation, once this matrix holds the factorial loadings which are the covariances between the factors and the original variables [13,14,24].
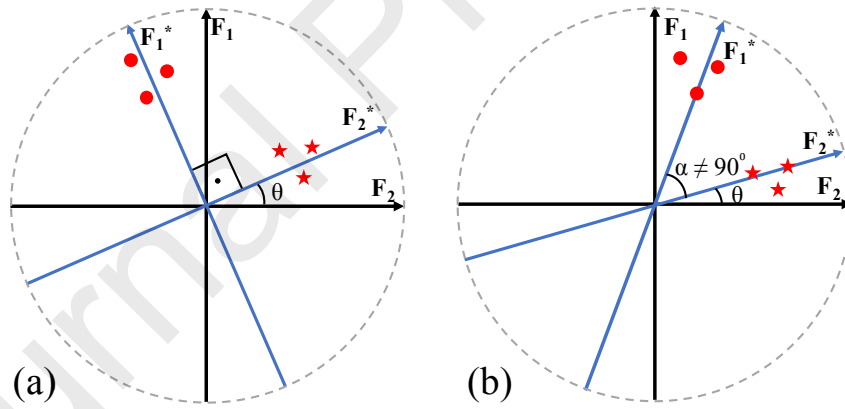

Fig. B.1. (a) orthogonal; and (b) oblique factor rotation

Figure B.1 illustrates the factor rotation in the factors space of unitary radius for the orthogonal case, Fig. B.1 (a) and in the oblique case Fig. B.1 (b). The rotated factor F_{1}^{*} explains the variables represented by circles, while the factor F_{2}^{*} explains the variables represented by stars. In the orthogonal case, there is no correlation between the rotated factors, while in the oblique case there is correlation between the rotated factors.

Several criteria have been proposed aiming to describe the correlations of the original variables through the factors in the simplest way. Taking a fixed origin, when rotating the axes from

F to $F^* = T^T F$, such that $L^* = LT$, with rotated loadings l_{ij}^*, despite the changes in the loadings, the commonalities remain constant, according to the Eq. B.1 [24,46].

$$h_i^2 = \sum_{j=1}^m l_{ij}^2 = \sum_{j=1}^m l_{ij}^{*\,2} = h_i^{*\,2} \tag{B.1}$$

The orthogonal matrix T, $T^T T = I$, must be found. Let the orthogonal rotation of two factors with the matrix T of order 2×2, considering the rotation angle θ measured in counterclockwise. It can be shown that the rotating matrix is in the form of the Eq. B.2. The orthogonal rotation is expressed through Eq. B.3 with the rotated loadings in Eq. B.4.

$$T = \begin{bmatrix} \cos\theta & -sen\,\theta \\ sen\,\theta & \cos\theta \end{bmatrix} \tag{B.2}$$

$$LT = \begin{bmatrix} l_{11} & l_{12} \\ l_{21} & l_{22} \\ \vdots & \vdots \\ l_{i1} & l_{i2} \\ \vdots & \vdots \\ l_{p1} & l_{p2} \end{bmatrix} \begin{bmatrix} \cos\theta & -sen\,\theta \\ sen\,\theta & \cos\theta \end{bmatrix} = \begin{bmatrix} l_{11}^* & l_{12}^* \\ l_{21}^* & l_{22}^* \\ \vdots & \vdots \\ l_{i1}^* & l_{i2}^* \\ \vdots & \vdots \\ l_{p1}^* & l_{p2}^* \end{bmatrix} = L^* \tag{B.3}$$

$$\begin{cases} l_{i1}^* = l_{i1} \times \cos\theta + l_{i2} \times \cos\theta \\ l_{i2}^* = -l_{i1} \times sen\,\theta + l_{i2} \times \cos\theta \end{cases} \tag{B.4}$$

Neuhaus and Wrigley [46] argued that the rotation aims to reduce the complexity of the description of the factors concentrating the variance of the variable in the lowest number of factors. The ideal rotation consisting of a one-factor pattern by variable in which its variance is represented by a single loading. They proposed to maximize the variance of the contribution of the factors. This criterion was called quartimax, since it maximizes the sum of the fourth-order powers of the elements of the rotated matrix. Considering L^* as the matrix of the loadings with the highest variances of the quadratic elements, the variance of L may be written according to the Eq. B.5.

$$qmax = \frac{\sum_{i=1}^p \sum_{j=1}^m l_{ij}^4}{pm} - \frac{\sum_{i=1}^p \left(\sum_{j=1}^m l_{ij}^2 \right)}{p^2 m^2} \tag{B.5}$$

Kaiser [47] proposed a variance criterion in which the variances for each factor, $j = 1, \ldots, m$, are summed constituting the varimax criteria, trying to maximize the interpretability or the simplicity of the factor, according to the Eq. B.6. He argued that the easy to interpret loadings are that nearby the extremes ±1 and that nearly 0, while the loadings nearby ±0.5 are difficult to interpret. The varimax criteria may also be rewritten considering the standardization due to the differences in the common variances, according to Eq. B.7.

$$vmax^* = \frac{1}{p^2} \Sigma_{j=1}^m \left[p\Sigma_{i=1}^p l_{ij}^4 - \left(\Sigma_{i=1}^p l_{ij}^2 \right)^2 \right] \tag{B.6}$$

$$vmax = \frac{1}{p^2} \Sigma_{j=1}^m \left[p\Sigma_{i=1}^p \left(l_{ij}^2/h_{ij}^2 \right)^2 - \left(\Sigma_{i=1}^p l_{ij}^2/h_{ij}^2 \right)^2 \right] \tag{B.7}$$

While the quartimax rotation maximizes the variance of the quadratic loadings among the factors, the varimax criterion maximizes the sum of the variance inside the factors.

APPENDIX C. RESULTS OF ASSUMPTIONS FOR GR&R ANOVA

To perform GR&R random effects ANOVA in the scores of the obtained factors the normality assumption of the residuals was checked for PA_1 and PA_2. The p-values for Shapiro-Wilk normality test were 0.6777 and 0.7382 for PA_1 and PA_2 respectively. Figure C.1 presents the residuals plots assuring normality distribution of the residuals for PA_1 and PA_2.

Residuals for PA1

Residuals for PA2
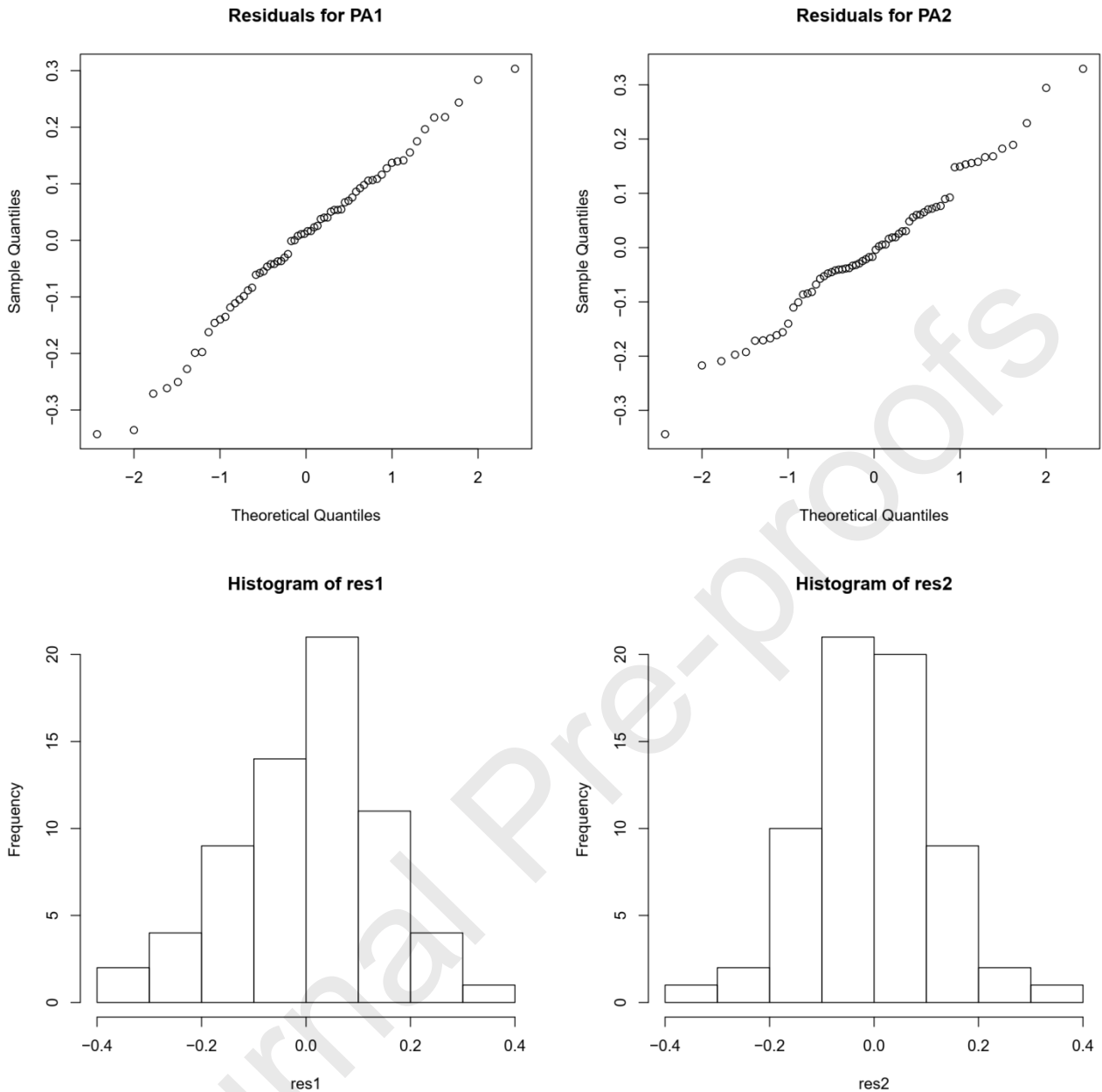
Histogram of res1

Histogram of res2

Fig. C.1. Residuals plots

APPENDIX D. VARIMAX ROTATION RESULTS

The rotation through varimax method was also implemented, however the quartimax results presented highest cumulative variance explanation. The factor analysis through principal axis extraction method with variamax rotation is summarized in Table D.1.

Table D.1. Factor analysis results, with principal axis extraction method and varimax rotation

	PA_1	PA_2	h_i^2	ψ_i	$Var(Y_i)$
Ron_p	-0.17	0.93	0.89	0.11	1.1
Ron_t	-0.05	0.99	0.99	0.01	1.0
Cyl_t	-0.03	0.94	0.88	0.12	1.0
R_a	0.99	-0.1	0.99	0.01	1.0
R_z	0.99	-0.11	0.99	0.01	1.0
R_q	0.99	-0.11	0.99	0.01	1.0
SS loadings	2.97	2.76			
Proportion Var	0.49	0.46			
Cumulative Var	0.49	0.95			

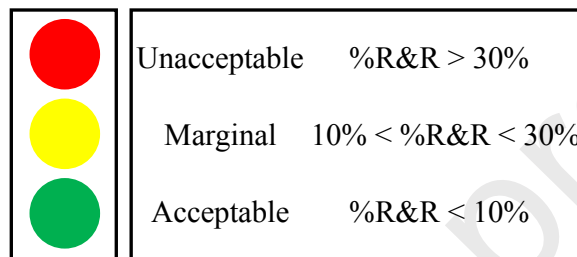|	
🔴	Unacceptable %R&R > 30%
🟡	Marginal 10% < %R&R < 30%
🟢	Acceptable %R&R < 10%

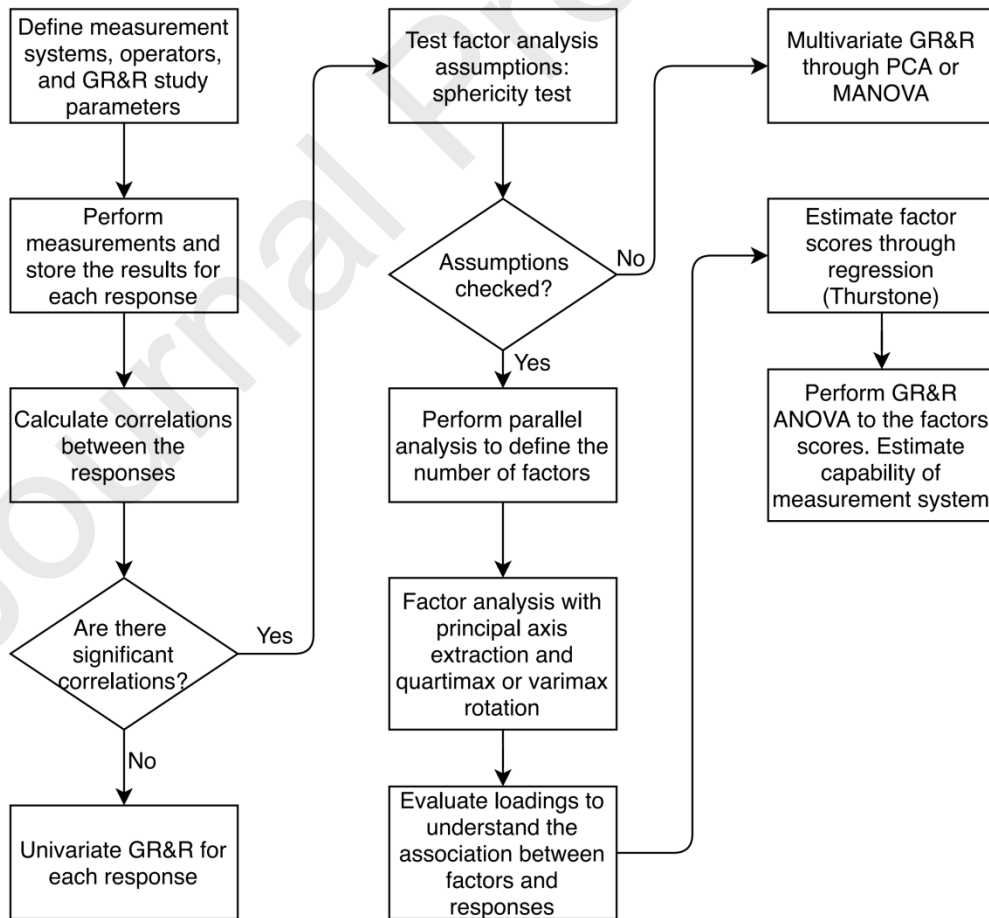Fig. 1. GR&R criteria for measurement system acceptability [7,18]

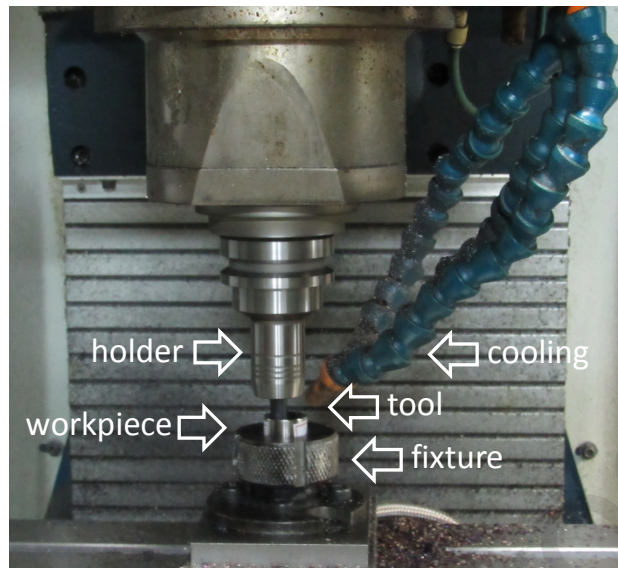Fig. 2. Flowchart for the GR&R-FA method

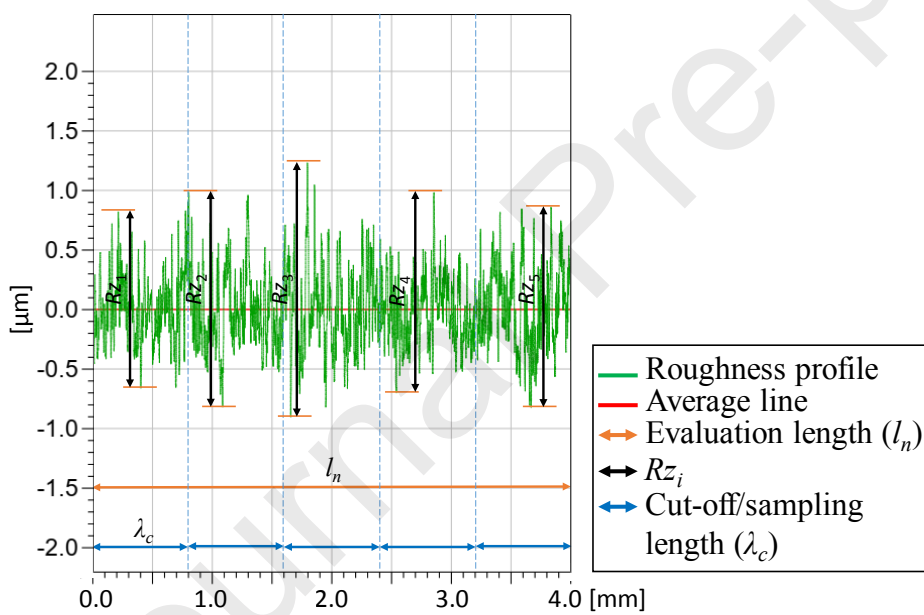Fig. 3. Experimental setup for the helical milling tests

Fig. 4. Roughness measurement terminology
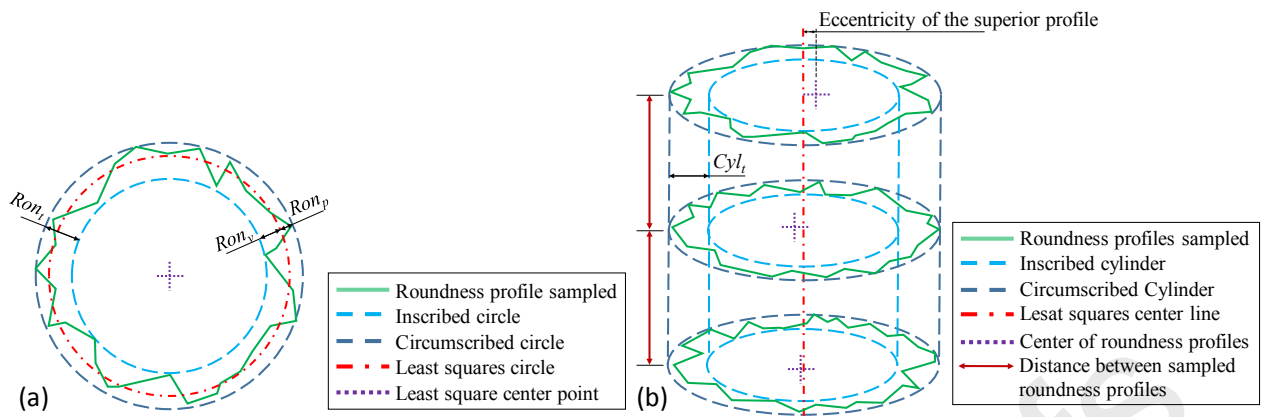
Fig. 5. (a) Roundness measurement; and (b) cylindricity measurement terminology
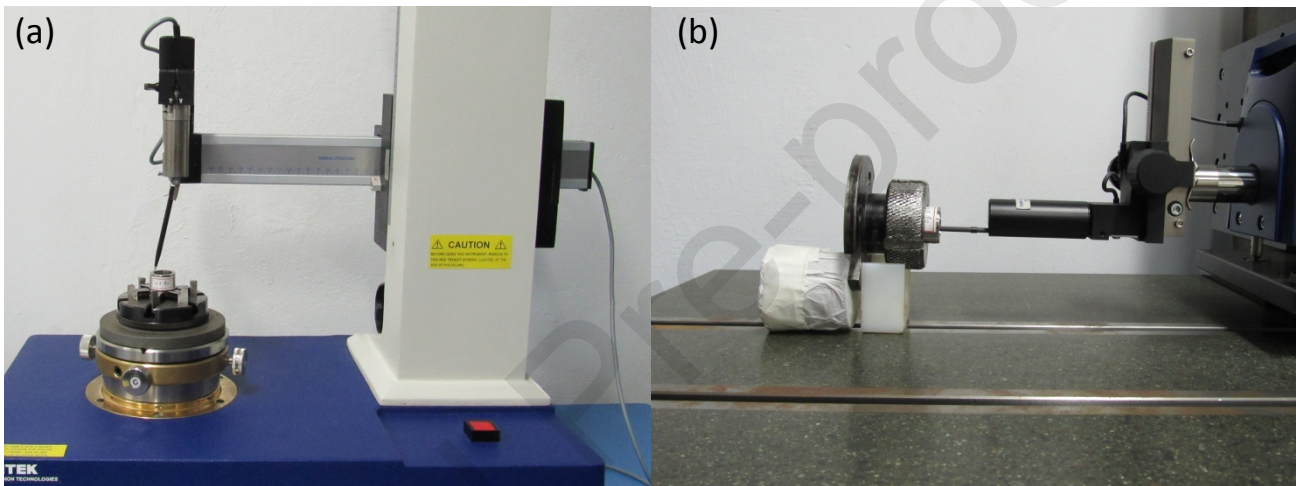
Fig. 6. Setup for (a) roundness; and (b) roughness measurements
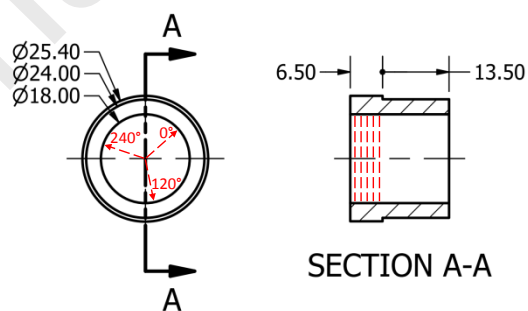
Fig.7. Roundness and roughness measurement positions
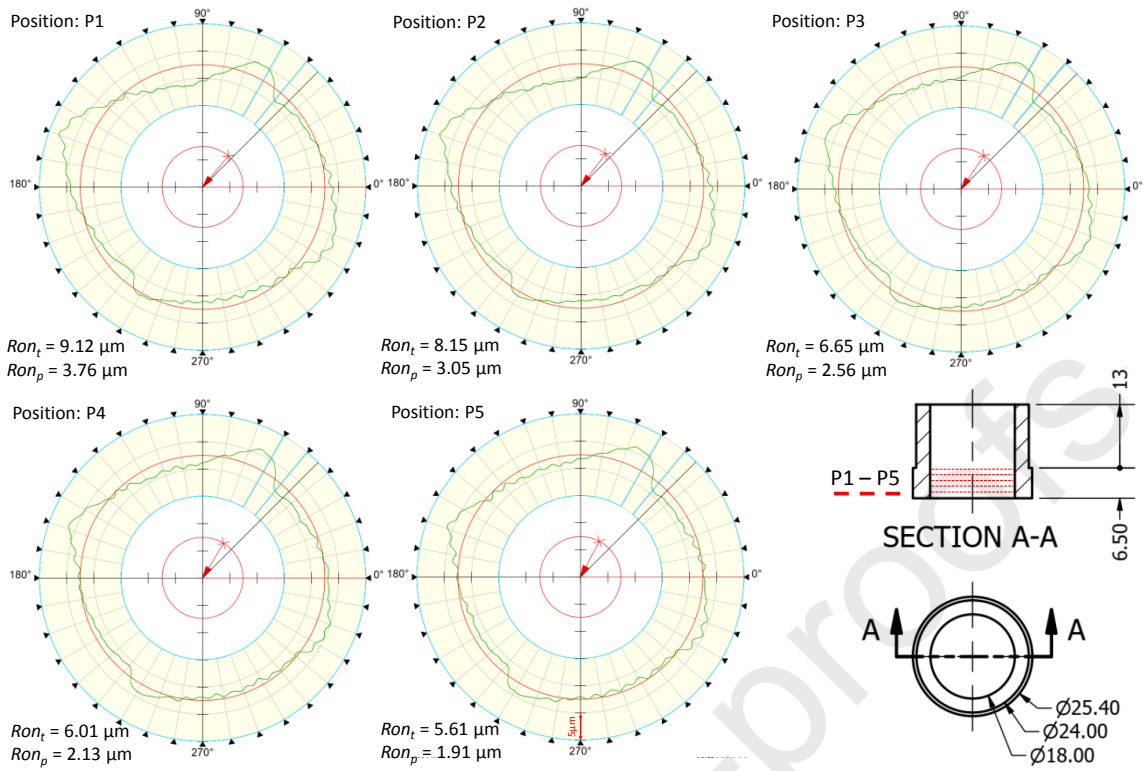
Position: P1

Ron_t = 9.12 µm
Ron_p = 3.76 µm

Position: P2

Ron_t = 8.15 µm
Ron_p = 3.05 µm

Position: P3

Ron_t = 6.65 µm
Ron_p = 2.56 µm

Position: P4

Ron_t = 6.01 µm
Ron_p = 2.13 µm

Position: P5

Ron_t = 5.61 µm
Ron_p = 1.91 µm

P1 – P5

SECTION A-A

Ø25.40
Ø24.00
Ø18.00

13

6.50

Fig. 8. Roundness measurements, part 1, operator 2, and replica 1. Ron_t = 7.11 µm, Ron_p =2.68 µm
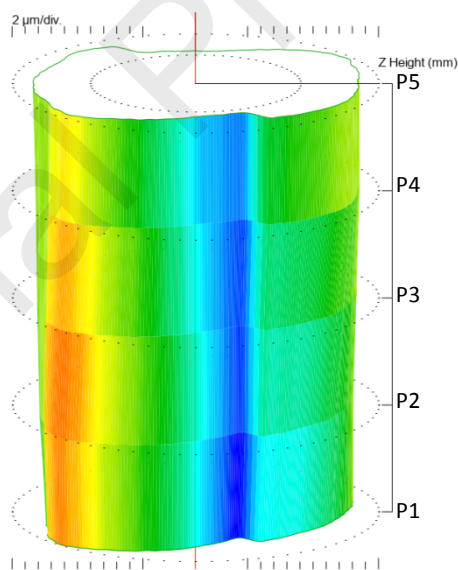
Fig. 9. Cylindricity measurement, part 2, operator 3, and replica 1. Cyl_t = 11.93 µm
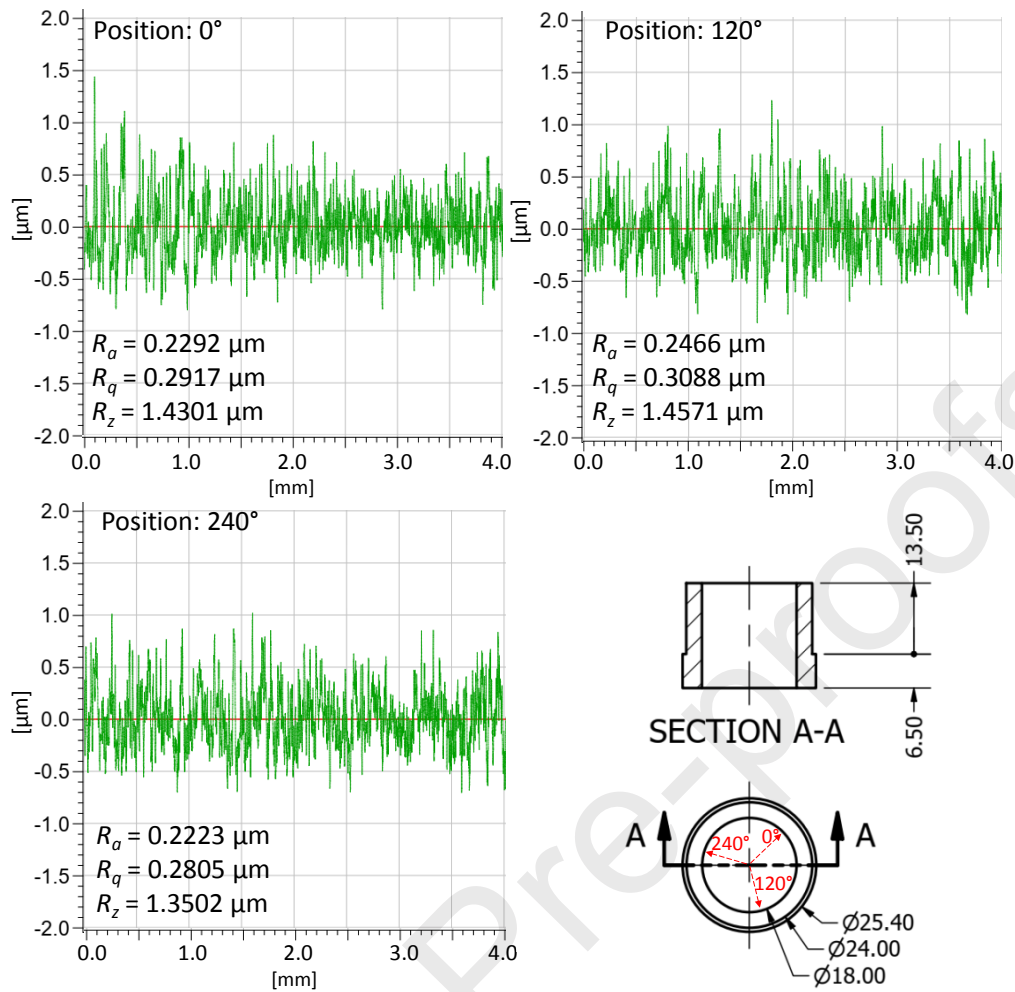
Fig. 10. Roughness measurements, part 3, operator 1, and replica 1. $R_a = 0.23$ μm, $R_q = 0.29$ μm, $R_z = 1.41$ μm;
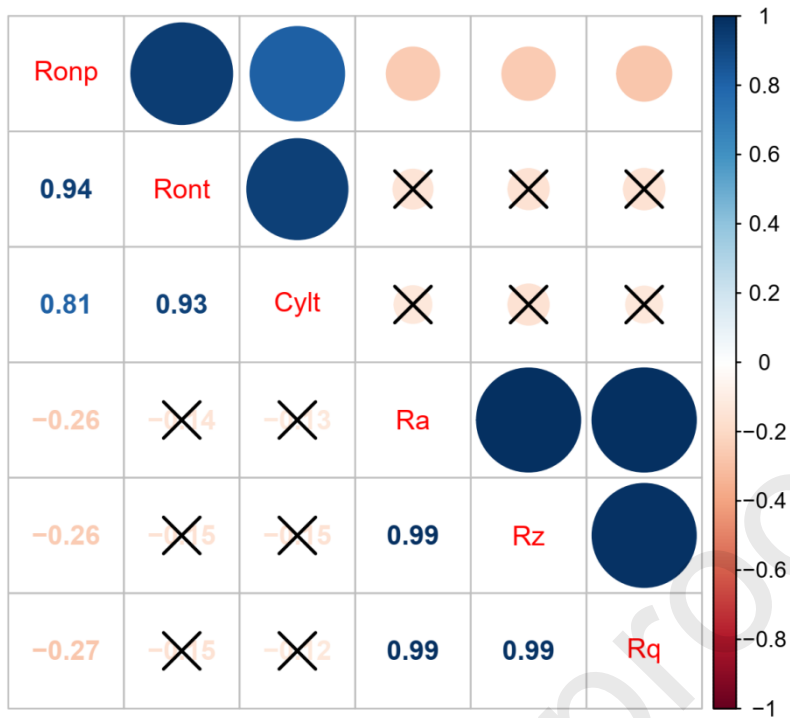
Fig. 11. Correlation plot for the variables of the GR&R study
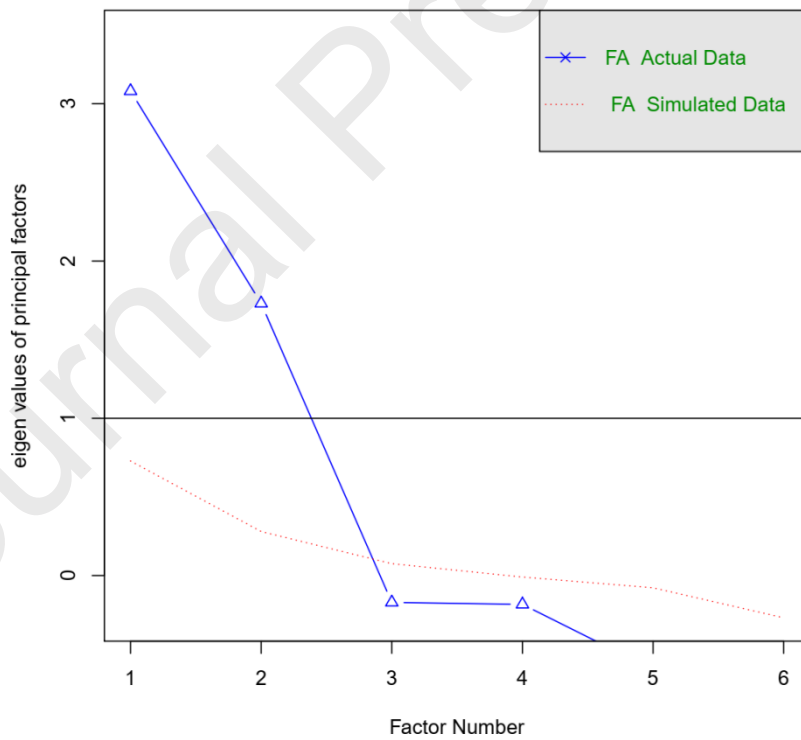
Fig. 12. Parallel analysis for principal axis extraction factor analysis
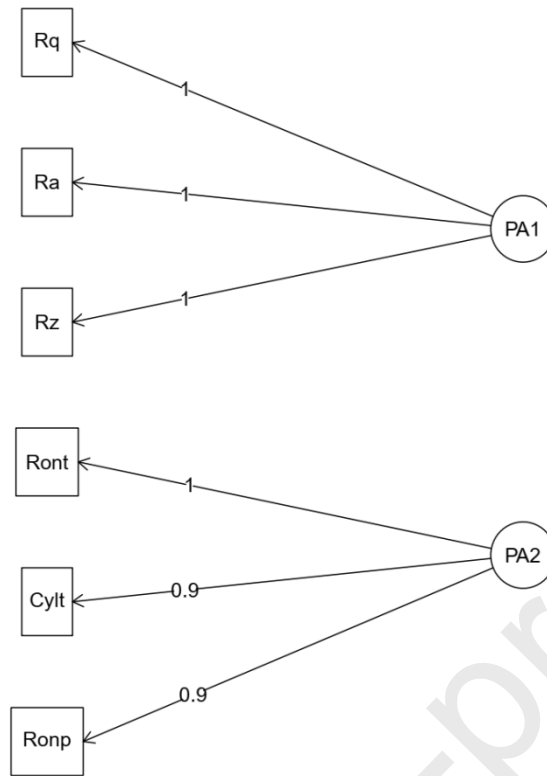
Fig. 13. Factor analysis diagram
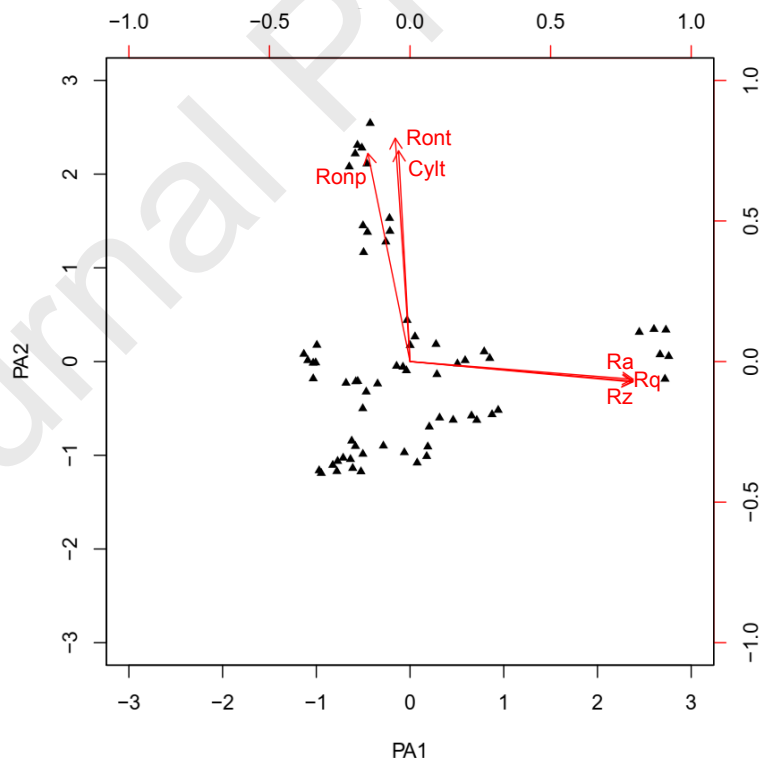
Fig. 14. Biplot for principal axis factor analysis with quartimax rotation
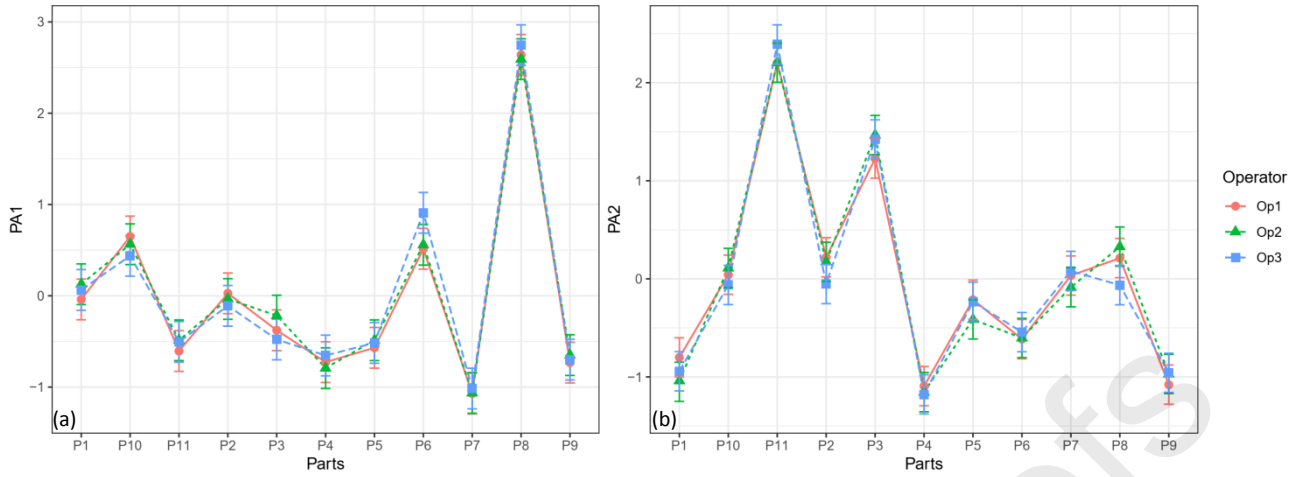
Fig. 15. Interaction plot for (a) PA_1; and (b) PA_2
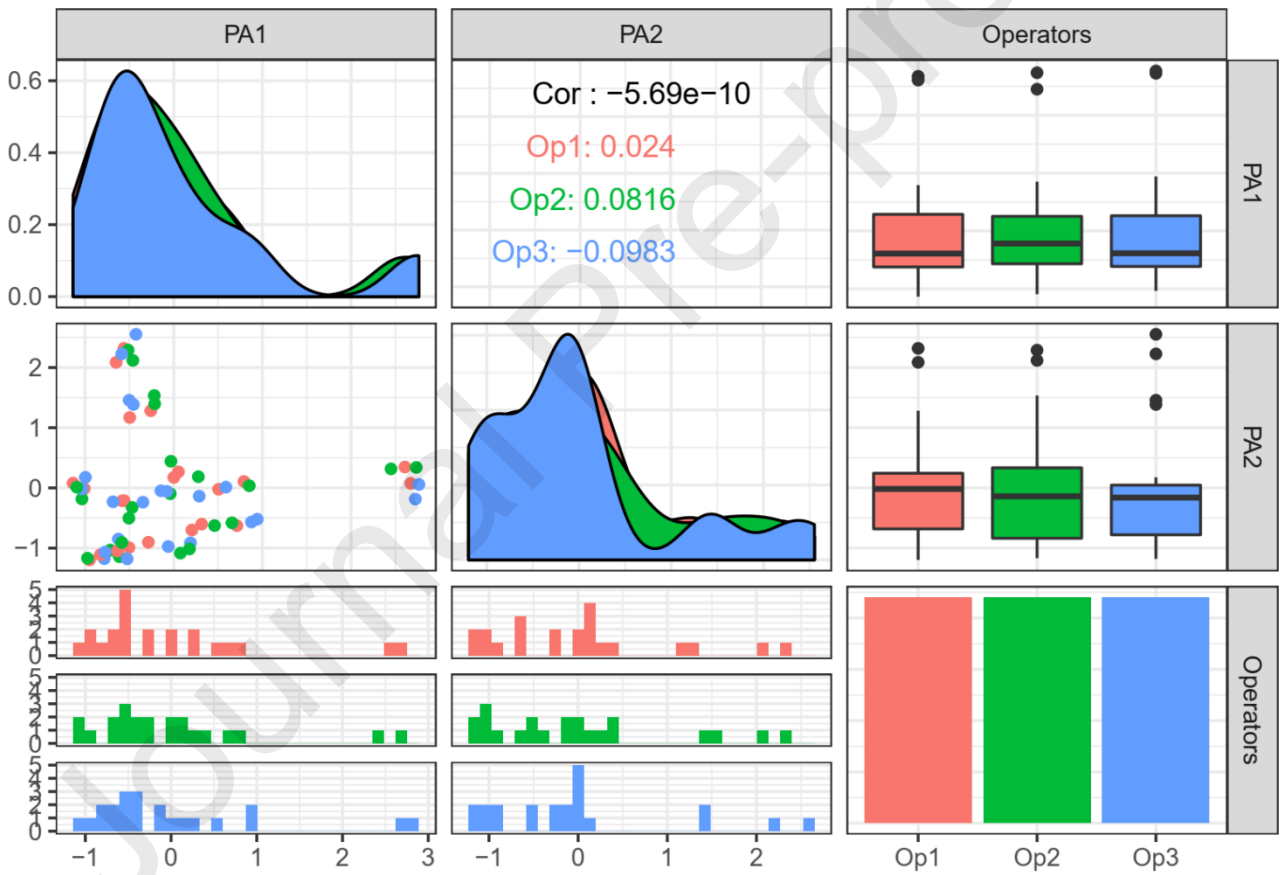
Fig. 16. Final outlook for the GR&R-FA method applied to the helical milling hole quality characterization

Fig. B.1. (a) orthogonal; and (b) oblique factor rotation

Residuals for PA1

Residuals for PA2

Histogram of res1

Histogram of res2
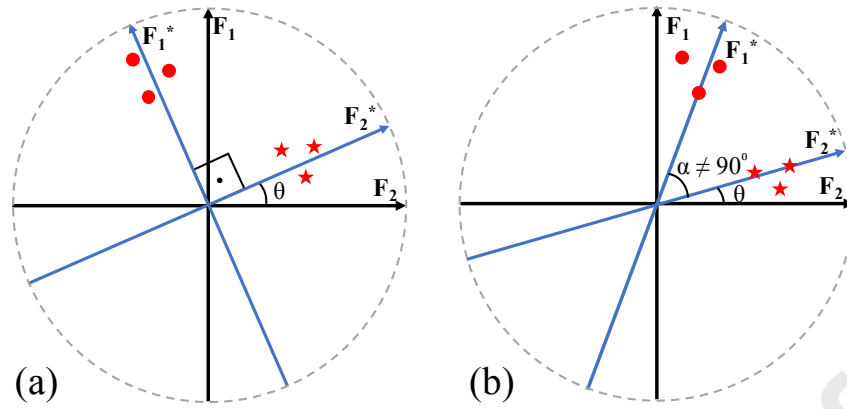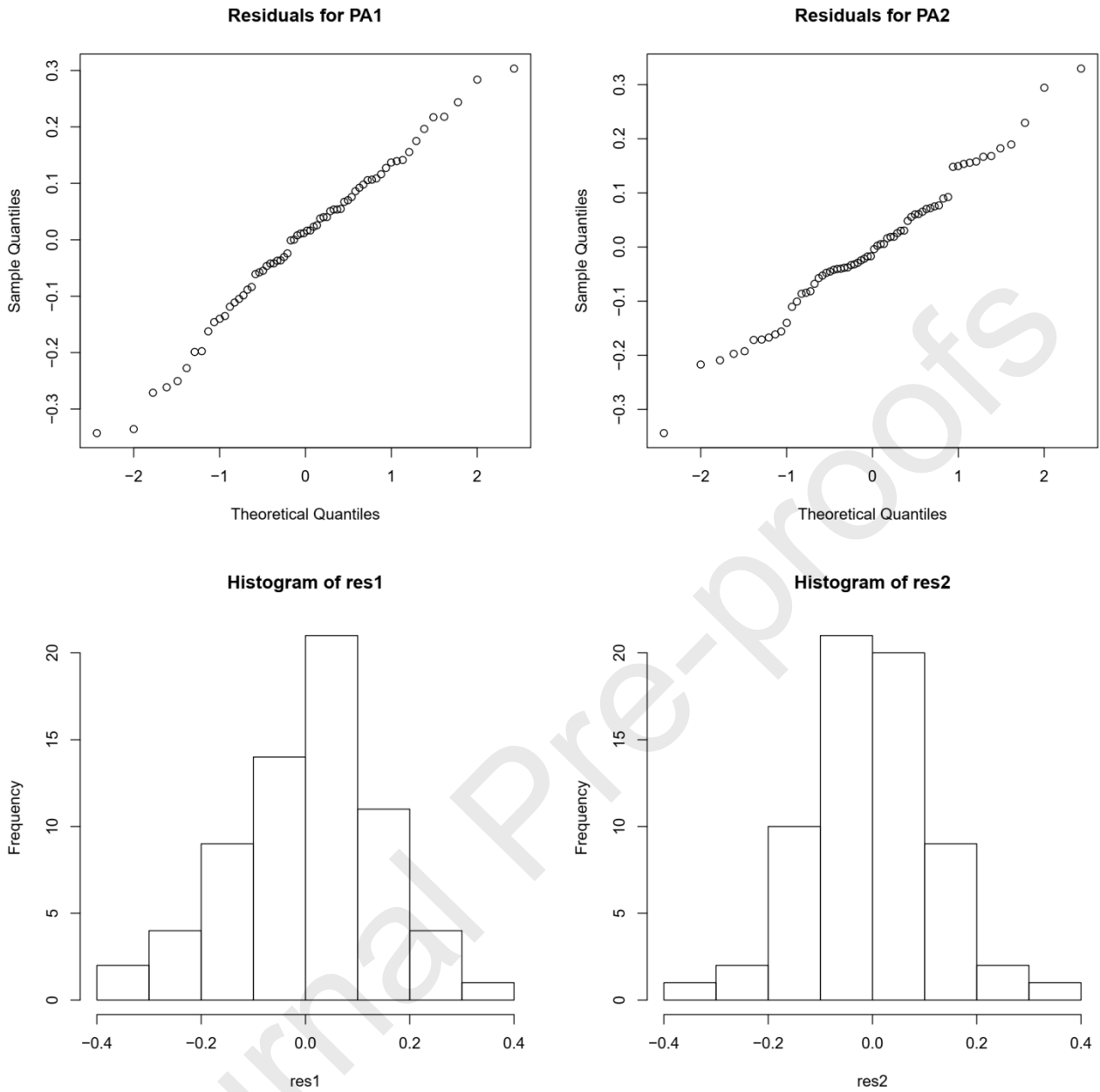
Fig. C.1. Residuals plots

Table 1. ANOVA table for a crossed GR&R study with two random factors

Sources	*Degrees of freedom*	*Mean square*	F_0
Parts (P)	$p - 1$	$\sigma_P^2 = \dfrac{or\sum_i(\bar{y}_{i..} - \bar{y}_{...})^2}{p - 1}$	$F_{0(P)} = \dfrac{\sigma_P^2}{\sigma_{PO}^2}$
Operators (O)	$o - 1$	$\sigma_O^2 = \dfrac{pr\sum_j(\bar{y}_{.j.} - \bar{y}_{...})^2}{o - 1}$	$F_{0(O)} = \dfrac{\sigma_O^2}{\sigma_{PO}^2}$

$P \times O$	$(p-1)(o-1)$	$\sigma_{PO}^2 = \dfrac{r\Sigma_i\Sigma_j(\bar{y}_{ij.} - \bar{y}_{i..} - \bar{y}_{.j.} + \bar{y}_{...})^2}{(p-1)(o-1)}$	$F_{0(PO)} = \dfrac{\sigma_{PO}^2}{\sigma_\varepsilon^2}$
Repeatability (ε)	$po(r-1)$	$\sigma_\varepsilon^2 = \dfrac{\Sigma_i\Sigma_j\Sigma_k(y_{ijk} - \bar{y}_{ij.})^2}{po(r-1)}$	

where $\bar{y}_{...}$ is the grand mean of the measurements; $\bar{y}_{i..}$ is the average of the ith part; $\bar{y}_{.j.}$ is the average of the jth operator; $\bar{y}_{ij.}$ is the average of the ith part measured by the jth operator and y_{ijk} is the kth measurement of the ith part by the jth operator

Table 2. Measurements for GR&R study, all results in [μm]

Parts	Operator	Replica 1						Replica 2					
		Ron_p	Ron_t	Cyl_t	R_a	R_z	R_q	Ron_p	Ron_t	Cyl_t	R_a	R_z	R_q
1	1	3.55	8.33	9.96	0.30	1.76	0.38	3.18	7.80	11.00	0.26	1.59	0.33
1	2	2.68	7.11	10.34	0.29	1.72	0.36	2.72	7.38	9.31	0.30	1.78	0.37
1	3	3.16	7.65	9.76	0.30	1.76	0.38	3.02	7.49	10.57	0.28	1.66	0.35
2	1	5.97	11.25	12.43	0.28	1.66	0.35	6.13	11.50	13.64	0.28	1.66	0.35
2	2	6.43	12.09	14.01	0.27	1.62	0.34	5.51	10.40	11.88	0.27	1.66	0.35
2	3	5.67	10.54	11.93	0.26	1.63	0.34	5.65	10.47	11.85	0.25	1.69	0.35
3	1	6.38	14.53	21.12	0.23	1.41	0.29	6.47	14.80	21.05	0.25	1.49	0.32
3	2	6.86	15.62	21.69	0.24	1.52	0.32	6.71	15.22	20.68	0.25	1.53	0.32
3	3	6.77	15.39	21.22	0.24	1.36	0.29	6.57	15.16	20.28	0.22	1.43	0.30
4	1	3.52	6.94	8.34	0.22	1.32	0.27	3.65	7.44	9.15	0.25	1.46	0.31
4	2	3.52	7.04	8.68	0.24	1.45	0.30	3.55	7.00	8.63	0.21	1.31	0.27
4	3	3.38	6.92	8.71	0.23	1.37	0.29	3.35	6.84	9.02	0.25	1.46	0.31
5	1	5.30	10.02	11.48	0.24	1.42	0.30	5.45	10.02	11.17	0.24	1.42	0.30
5	2	5.18	9.61	11.99	0.25	1.45	0.31	4.98	9.11	10.84	0.24	1.47	0.31
5	3	5.30	9.86	10.94	0.26	1.50	0.32	5.41	10.04	11.09	0.23	1.39	0.29
6	1	3.78	8.16	12.51	0.28	1.76	0.41	3.76	8.16	11.47	0.34	1.87	0.43
6	2	3.73	8.11	12.43	0.32	1.76	0.42	3.83	8.27	13.01	0.33	1.85	0.43
6	3	3.80	8.15	12.57	0.34	1.93	0.46	3.85	8.31	11.18	0.35	1.93	0.46
7	1	6.37	10.86	15.07	0.20	1.28	0.25	6.47	11.19	14.19	0.19	1.23	0.24
7	2	5.71	10.29	12.34	0.20	1.27	0.25	6.37	10.89	13.07	0.20	1.22	0.25
7	3	6.32	10.83	14.55	0.20	1.26	0.25	6.69	11.49	14.57	0.20	1.29	0.25
8	1	5.28	11.36	13.04	0.47	2.68	0.59	4.71	10.49	12.37	0.48	2.72	0.60
8	2	5.10	11.25	13.42	0.47	2.60	0.58	5.11	11.29	12.99	0.49	2.71	0.60
8	3	4.50	9.56	11.27	0.49	2.73	0.61	4.67	10.24	11.77	0.50	2.69	0.61
9	1	3.01	7.14	9.91	0.22	1.37	0.28	3.12	7.30	9.19	0.24	1.42	0.30
9	2	3.26	7.43	8.45	0.23	1.41	0.29	3.33	7.68	9.07	0.24	1.42	0.31
9	3	3.56	7.98	10.21	0.24	1.43	0.30	3.10	7.24	8.79	0.23	1.36	0.29
10	1	4.03	10.14	16.73	0.30	1.82	0.42	4.19	10.44	16.43	0.34	1.85	0.44
10	2	4.56	10.94	18.21	0.30	1.68	0.38	4.22	10.26	16.47	0.36	1.86	0.44
10	3	4.17	10.33	16.86	0.33	1.82	0.41	4.19	9.96	16.95	0.30	1.72	0.38
11	1	9.00	18.26	22.75	0.22	1.33	0.28	8.61	17.52	21.87	0.22	1.30	0.27
11	2	8.80	18.10	22.60	0.23	1.33	0.29	8.65	17.61	21.82	0.23	1.38	0.29
11	3	9.32	18.94	22.96	0.23	1.36	0.29	8.80	17.94	22.96	0.22	1.32	0.28

Table 3. Correlation matrix

	Ron_p	Ron_t	Cyl_t	R_a	R_z
Ron_t	0.944 [a]				
	0.000 [b]				
Cyl_t	0.813	0.932			
	0.000	0.000			
R_a	-0.256	-0.142	-0.127		

Table 4. Factor analysis results, with principal axis extraction method and quartimax rotation

	PA_1	PA_2	h_i^2	ψ_i	$Var(Y_i)$
Ron_p	-0.19	0.93	0.89	0.11	1.0
Ron_t	-0.07	0.99	0.99	0.01	1.0
Cyl_t	-0.05	0.94	0.88	0.12	1.0
R_a	0.99	-0.08	0.99	0.01	1.0
R_z	0.99	-0.09	0.99	0.01	1.0
R_q	0.99	-0.09	0.99	0.01	1.0
$Var(PA_j)$	2.99	2.74			
Proportion Var	0.5	0.46			
Cumulative Var	0.5	0.96			

Table 5. Scores of the factors PA_1 and PA_2

		Replica 1		Replica 2				Replica 1		Replica 2	
Parts	Operator	PA_1	PA_2	PA_1	PA_2	Parts	Operator	PA_1	PA_2	PA_1	PA_2
1	1	0.205	-0.700	-0.285	-0.904	7	1	-1.009	-0.012	-1.135	0.080
1	2	0.078	-1.063	0.177	-1.016	7	2	-1.035	-0.183	-1.093	0.012
1	3	0.189	-0.913	-0.061	-0.975	7	3	-1.036	-0.016	-0.996	0.176
2	1	0.001	0.174	0.053	0.266	8	1	2.607	0.347	2.672	0.076
2	2	-0.031	0.443	-0.039	-0.096	8	2	2.450	0.316	2.735	0.340
2	3	-0.144	-0.048	-0.076	-0.058	8	3	2.725	-0.186	2.765	0.057
3	1	-0.496	1.170	-0.258	1.283	9	1	-0.826	-1.111	-0.637	-1.048
3	2	-0.219	1.536	-0.215	1.397	9	2	-0.715	-1.034	-0.584	-0.908
3	3	-0.502	1.457	-0.455	1.386	9	3	-0.624	-0.851	-0.775	-1.068
4	1	-0.949	-1.197	-0.505	-0.992	10	1	0.507	-0.023	0.793	0.107
4	2	-0.613	-1.144	-0.972	-1.169	10	2	0.278	0.186	0.852	0.036
4	3	-0.783	-1.177	-0.525	-1.180	10	3	0.589	0.012	0.287	-0.138
5	1	-0.559	-0.211	-0.580	-0.214	11	1	-0.561	2.319	-0.649	2.088
5	2	-0.468	-0.325	-0.506	-0.504	11	2	-0.514	2.290	-0.460	2.119
5	3	-0.347	-0.238	-0.684	-0.231	11	3	-0.425	2.554	-0.585	2.227
6	1	0.316	-0.602	0.713	-0.628						
6	2	0.461	-0.626	0.657	-0.580						
6	3	0.876	-0.566	0.942	-0.520						

Table 6. GR&R ANOVA

GR&R ANOVA for PA_1					
	Df	Sum Sq	Mean Sq	F-value	p-value
Parts	10	63.67	6.367	257.847	<2e-16
Operators	2	0.02	0.012	0.475	0.625
Repeatability	53	1.31	0.025		
Total	65	65.00			

GR&R ANOVA for PA_2					
	Df	Sum Sq	Mean Sq	F-value	p-value
Parts	10	63.94	6.394	321.498	<2e-16
Operators	2	0.01	0.004	0.181	0.835
Repeatability	53	1.05	0.020		
Total	65	65.00			

Table 7. Variance components contribution

Contribution for PA_1			
	StdDev	StudyVar	%StudyVar
Total R%R	0.157	0.943	15.11
Repeatability	0.157	0.943	15.11
Reproducibility	0.000	0.000	0.00
Operators	0.000	0.000	0.00
Part-To-Part	1.028	6.169	98.85
Total	1.040	6.240	100.00
Contribution for PA_2			
	StdDev	StudyVar	%StudyVar
Total R%R	0.141	0.846	13.56
Repeatability	0.141	0.846	13.56
Reproducibility	0.000	0.000	0.00
Operators	0.000	0.000	0.00
Part-To-Part	1.031	6.184	99.08
Total	1.040	6.242	100.00

Table 8. Gage capability indexes

Index	PA_1	PA_2
SNR(ndc)	9	10
DR	9.31	10.38

Table D.1. Factor analysis results, with principal axis extraction method and varimax rotation

	PA_1	PA_2	h_i^2	ψ_i	Var(Y_i)
Ron_p	-0.17	0.93	0.89	0.11	1.1
Ron_t	-0.05	0.99	0.99	0.01	1.0
Cyl_t	-0.03	0.94	0.88	0.12	1.0
R_a	0.99	-0.1	0.99	0.01	1.0
R_z	0.99	-0.11	0.99	0.01	1.0
R_q	0.99	-0.11	0.99	0.01	1.0
SS loadings	2.97	2.76			
Proportion Var	0.49	0.46			
Cumulative Var	0.49	0.95			

Highlights

1. A multivariate GR&R method through factor analysis is proposed.

2. GR&R-FA method presented a simple interpretation of the highly correlated groups.

3. Quality measurements of holes attained by helical milling validated the method.

4. Roughness and roundness parameters were measured in the investigation.